2015

New physics at the weak scale: axigluon models, scale invariance and naturalness, and interacting dark matter

BOSTON UNIVERSITY

GRADUATE SCHOOL OF ARTS AND SCIENCES

Dissertation

NEW PHYSICS AT THE WEAK SCALE: AXIGLUON MODELS, SCALE INVARIANCE AND NATURALNESS, AND INTERACTING DARK MATTER

by

GUSTAVO MARQUES TAVARES

B.Sc., Universidade Estadual de Campinas, Campinas, SP, Brazil, 2008
M.Sc., Universidade Estadual de Campinas, Campinas, SP, Brazil, 2010

Submitted in partial fulfillment of the
requirements for the degree of
Doctor of Philosophy
2015

Approved by

First Reader

Martin Schmaltz, Ph.D.
Professor of Physics

Second Reader

Andrew Cohen, Ph.D.
Professor of Physics

To Maira, with love.

Acknowledgments

There are many people I would like to thank, which in a way or another were very important in the making of this thesis.

First, I would like to thank my advisor Martin Schmaltz for his advice, guidance and friendship during my years in graduate school. I have learned a lot about physics and most importantly how to think about physics from him. He knew when to push me to work harder and also when to give me more space such that I could develop my academic independence, and I am really grateful for that. I am very thankful for him letting me tag along in different workshops and conferences, which allowed me to meet many other great physicist. And also for taking me sailing and to what he would consider very light hikes, which for me were usually strenuous but a lot of fun.

I would also like to thank the other Professors in the High Energy Theory group for their support during my studies. I am particularly thankful to Andy and Ami, who taught me a lot about field theory and who gave me interesting projects to work on during my doctoral training. The daily lunch conversations with Andy have taught me more Physics than most classes I have taken, and I am very grateful for this.

I am very thankful to my officemate, collaborator and good friend Yiming Xu. I have learned a lot by talking to her and having a good friend by my side at work made things a lot more fun.

I would also like to thank the other people in the group, Evan, Matt, Siavosh and Zuhair. It was great to have had young smart people to talk to and learn from in the group. I am particularly indebted to Matt and Zuhair for sitting through some of my practice talks and giving me career advice when I was applying for postdocs. I also thank Mirtha for always being so helpful and friendly.

I cannot imagine my years in Boston without the great friends I have made while here. I am very thankful for having met Alex, Colin, Maria and Tina, with whom I shared some

of the best moments during my time in Boston and who I hope will always be part of my life. I was also very fortunate to have Gustavo and Joao, who had been my roommates and good friends back in Brazil move to Boston while I was here.

I will be forever thankful to my family for giving my incredible support through my life. I am very thankful to my father and his wife Lia for always encouraging me in my graduate studies and for all the help when I first moved to Boston. I am also very grateful to my godfather Ruy (Psit) who was the first person to teach me the importance of knowledge and for having been a role model to me when I was a kid. And, of course, I would like to specially thank my Mom, who I know hated seeing her son move to another country, but nonetheless wholeheartedly supported my decision to come to Boston for my PhD.

Finally, I would like to thank my wife-to-be Maira with whom I have shared all the victories and who has helped me through all the hard times of the last many years of our lives. I thank her for being such an awesome partner and great company in the various adventures we have had together. I am incredibly lucky to have such an amazing person by my side.

NEW PHYSICS AT THE WEAK SCALE: AXIGLUON MODELS, SCALE INVARIANCE AND NATURALNESS, AND INTERACTING DARK MATTER

(Order No.)

GUSTAVO MARQUES TAVARES

Boston University Graduate School of Arts and Sciences, 2015

Major Professor: Martin Schmaltz, Professor of Physics

ABSTRACT

The Standard Model of particle physics describes all known elementary particles and their interactions. Despite its great experimental success, we know that the Standard Model is not a complete description of Nature and therefore new phenomena should be observed at higher energies. In the coming years the Large Hadron Collider will test the Standard Model by colliding protons with center of mass energies of up to 14 TeV providing some of the most stringent tests on the Standard Model.

Experimental searches for Dark Matter provide a complementary program to test physics at the weak scale. In the near future new experimental data coming from direct detection experiments, and from satellites and telescopes will drastically improve our sensitivity to weak scale dark matter. This could lead to the first direct observation of dark matter, and thus of physics beyond the Standard Model.

In this thesis I propose different extensions of the Standard Model and discuss their experimental consequences. I first discuss models for Axigluons, which are spin one particles in the adjoint representation of the SU(3) color gauge group. These models were motivated by the measurement of higher than predicted forward-backward asymmetry in top quark pair production at the Tevatron. I study different scenarios for Axigluon models that can explain the Tevatron result and explore their signatures at the Large Hadron Collider.

Second I discuss the implications of ultraviolet scale invariance for the Standard Model, which has been advocated as a solution to the hierarchy problem. I show that in order to solve the hierarchy problem with scale invariance, new physics is required not far from the weak scale. In the last part of this thesis I propose a new model for dark matter, in which dark matter is charged under a hidden non-Abelian gauge group. This leads to modifications in the sensitivity of the usual experimental searches for dark matter in addition to distinct signatures in the Cosmic Microwave Background and in Large Scale Structure data.

Contents

List of Figures

List of Abbreviations

A_{FB}	Forward-Backward Asymmetry
CFT	Conformal Field Theory
DM	Dark Matter
DR	Dark Radiation
EFT	Effective Field Theory
eV	Electron Volt
IR	Infrared
LHC	Large Hadron Collider
LO	Leading Order
NLL	Next to Leading Logarithm
NLO	Next to Leading Order
NNLO	Next to Next to Leading Order
QCD	Quantum Chromodynamics
SM	Standard Model
UV	Ultraviolet
WIMP	Weakly Interacting Massive Particle

1 Introduction

1.1 Overview

1.1.1 Overview

This thesis was written during a very interesting time in Particle Physics. In 2012, The Large Hadron Collider (LHC) discovered the last missing piece of the Standard Model of Particle Physics, the Higgs boson [5, 6]. This confirmed that the Standard Model (SM), which was developed more than three decades ago [7–9], is a consistent description of elementary particle physics that can be extrapolated up to the Planck Scale, where quantum gravity must be taken into account.

The modern interpretation of the Standard Model is that it is an effective field theory which is valid description of physics beyond some cutoff energy scale at which new physics appears. For energies near the Planck scale we know it must be replace by a more fundamental theory which includes quantum gravity effects and at much lower energies it needs to be modified to include dark matter. Despite the fact that we have no experimental evidence for what the cutoff scale of the SM is, there are various theoretical motivations that point to it being not far from the Weak scale (200 GeV). Two of the strongest motivations for new physics near the Weak scale are the hierarchy problem in the Standard Model and the WIMP (Weakly Interacting Massive Particle) miracle for dark matter, which will be explained in the next subsections. On the other hand, departures from the SM could appear at unexpected places as has been the case in the past, and thus it is important to make sure that the different experiments are not missing potentially interesting signals.

There is a wealth of new data coming from the LHC, from various experiments searching for dark matter and also from astrophysics and cosmology experiments. Up to this point no sign of new physics has been seen, which has led the community to question the idea of naturalness, which has been used as one of the main guides in building models of new

physics in the past few decades. This new data has also probed a large fraction of the parameter space for weak scale dark matter without a convincing positive signal. In addition, data from the Planck satellite combined with other astrophysical surveys have measured the parameters of the Standard Cosmological Model (ΛCDM) to unprecedented precision, providing a very good picture for the evolution of our universe.

In this thesis I study three different scenarios for physics beyond the Standard Model. First I study Axigluon models, which were motivated by a longstanding discrepancy between the top quark forward-backward asymmetry measured at the Tevatron and the SM predictions. Next I study the implications of solving the hierarchy problem by modifying the SM in the ultraviolet such that it asymptotes a scale invariant theory. In the last part of the thesis I study a new type of dark matter model, in which dark matter carries an additional non-Abelian hidden gauge interaction, which modifies the sensitivity of dark matter searches and also leaves imprints in the Cosmic Microwave Background and in the matter power spectrum.

1.1.2 Axigluons and the Top Quark Forward-Backward Asymmetry

The top quark (top for short) is the heaviest particle in the Standard Model, with a mass around $m_t = 173$ GeV. Because it is heavy the top decays before hadronization, allowing us to distinguish it from other colored particles (gluons and all other quarks) produced in a collider, which all appear as a jet (a spray of hadronic particles). Almost all top quarks decay to a bottom quark and a positively charged W boson (W^+), while the anti-top decays to an anti-bottom and a W^-. The W boson is also unstable and decays to a quark anti-quark pair, which is called a hadronic decay, or to a lepton and a neutrino, called the leptonic decay. If a top (or anti-top) decays to a lepton one can determine wether it was a top or an anti-top by measuring the charge of the associated lepton.

The top quark forward-backward asymmetry is a measurement at a proton anti-proton ($p\bar{p}$) collider of the frequency in which a top is produced in the same direction as the incoming proton as opposed to the direction of the anti-proton. The leading contribution

to top quark pair production in a $p\bar{p}$ collider, dominated by the diagram in Figure 1.1 at the Tevatron, does not contribution to the asymmetry, which is generated by the next to leading order (NLO) contributions.

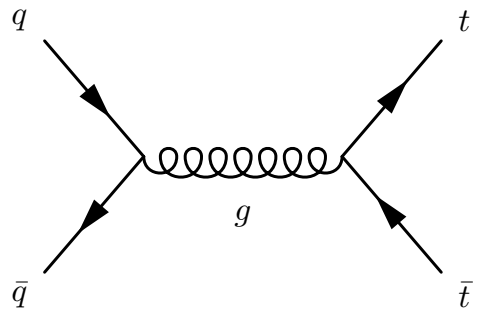

Figure 1.1: Leading contribution to the $t\bar{t}$ production at the Tevatron. At the same order in QCD there are also other diagrams contributing to $t\bar{t}$ production, but they have gluons in the initial state and are suppressed by the gluon parton distribution functions at energies above the production threshold.

This measurement has been performed by the CDF and D0 collaborations at the Tevatron accelerator. Both collaborations found a larger value for the asymmetry than the Standard Model prediction with around $3\,\sigma$ significance [10, 11]. This led to a large number of proposals of extensions of the Standard Model that could explain the large asymmetry. The best fit to the top data is obtained by a light Axigluon, which I proposed with M. Schmaltz [12] as an explanation for the forward-backward asymmetry.

An axigluon is a spin one particle which is in the adjoint representation of the Quantum Chromodynamics (QCD) gauge group, and that has a chiral coupling to quarks. Because it is charged under QCD it has a very large pair production cross-section at a hadron collider. In a paper with C. Gross, C. Spethmann and M. Schmaltz [13] I explored the LHC signatures for axigluon models that could explain the large asymmetry measured at the Tevatron. This work is described in Chapter 2 of this thesis, where I present a set of four example models differing in the way the axigluon decay to SM particles. Monte carlo implementations of these models are publicly available in order to help experimentalist in searches for axigluons at the LHC.

1.1.3 Scale Invariance in the Ultraviolet and Naturalness

The Naturalness argument is one of the main motivations for extensions of the Standard Model. The usual argument is that if one calculates corrections to the Higgs mass squared in perturbation theory one finds that these corrections depend on the cutoff squared. This points to the fact that the Higgs mass operator, which is not protected by any symmetry in the Standard Model, is highly sensitive to ultraviolet (high energy) physics. Given this sensitivity, it is expected that the Higgs mass itself should be proportional to the cutoff, unless there is very finely tuned cancelations between the mass parameter and the higher order corrections that yield a mass parametrically smaller than the cutoff.

There is no reason to expect such a conspiracy between the actual mass parameter and the corrections to the Higgs mass, which are proportional to the various couplings between the Higgs and other SM particles, and this has been named the Hierarchy problem. A large theoretical effort has gone into trying to make the low value of the Higgs mass "natural", generally by embedding the Standard Model in a theory with extra symmetries that protect the Higgs mass. The most compelling solutions invoke either supersymmetry (see e.g. [14]) or compositeness (see e.g. [15]). In both cases new colored particles are required with masses close to the Higgs mass. Such particles are one of the main targets of LHC searches. The results from run 1 of the LHC have placed strong bounds on such colored particles, leaving little space for supersymmetry or composite models as solutions to the Hierarchy problem.

This has led many people to search for new solutions to the Hierarchy problem. An idea that has received a lot of attention is to evoke scaling symmetry as a protection mechanism to the Higgs mass [16]. The idea is that if the Standard Model is approximately scale invariant, with scaling symmetry being restored in the ultraviolet, than the Higgs mass, which explicitly breaks scale invariance, would be protected from cutoff sensitivity by this symmetry.

The Standard Model, even if the Higgs mass is set to zero, is not scale invariant. A manifestation of this is the running of the couplings. Therefore, in order to evoke scale

invariance as a solution to the Hierarchy problem, one would need all couplings in the Standard Model to approach fixed points at high energies, such that the model asymptotes a scale invariant theory. In Chapter 3, I discuss the physical consequences of such a scenario and show that in order to solve the Hierarchy problem it requires departures from the SM not far from the weak scale. This Chapter is based on a paper written in collaboration with M. Schmaltz and W. Skiba [17].

1.1.4 Non-Abelian Dark Matter

We know that the particles in the Standard Model is correspond to only one fifth of the energy content in matter in the Universe. The remaining energy is in the form of a non-luminous component which we call dark matter (DM). We have overwhelming evidence for dark matter, coming from independent measurements ranging from analysis of galactic rotation curves to precision analysis of the Cosmic Microwave Background. On the other hand, all the evidence for dark matter comes from its gravitational effects and thus we know very little about it except for information on its energy density and that it does not interact significantly with light.

A very appealing class of models for dark matter models is that DM is a WIMP (Weakly Interacting Massive Particle). As the name suggest, in this models dark matter is a massive particle whose interaction cross-section with the Standard Model particles is similar to typical Weak scale interaction cross-sections. In the early Universe, when temperatures where much higher than the Weak scale, such interactions are large enough to keep dark matter at chemical and kinetic equilibrium with the Standard Model plasma. As the temperature drops due to the expansion it eventually becomes smaller than the dark matter mass. At this point the dark matter number density starts dropping exponentially,

$$n_\chi \propto \exp(-M_\chi/T).$$

If this process continued indefinitely the dark matter abundance would be completely depleted today and would not be able to account for the effects we have observed unless

it was produced through some other mechanism. This depletion takes place through the annihilation process DM DM $\rightarrow$ SM SM, which is proportional to the DM number density and hence becomes exponentially suppressed once the temperature drops below the dark matter mass. Once the rate for this process becomes small compared to the relevant time scale, which is given by the Hubble expansion rate H, the number density of dark matter freezes-out and is only diluted by the expansion of the universe (which changes the volume of a given region but not the number of dark matter in a given region). For a wide range of masses and annihilation cross-sections the abundance of dark matter today if it was produced via thermal freeze-out is approximately given by [18]

$$\Omega_{DM} h^2 \sim \frac{10^{-37}\mathrm{cm}^2}{\langle \sigma v \rangle_{\mathrm{annih}}}\,, \tag{1.1}$$

where Ω_{DM} is the ratio of the energy density in dark matter today divided by the critical density $\rho_{crit} = 3H^2/8\pi G$ and h is a dimensionless measure of the Hubble constant today, $H_0 = 100h\,\mathrm{km\ sec}^{-1}\,\mathrm{Mpc}^{-1}$. One interesting consequence of Eq. 1.1 is that the energy density is approximately determined by just the annihilation cross-section of DM into SM at the time of freeze-out. A surprising result is that for dark matter with mass around the weak scale ($M_\chi \sim 100\,\mathrm{GeV}$), and with typical weak interaction cross-section $\sigma \sim \alpha_w^2/M_\chi^2$, Eq. refeq:intro-freeze-out predicts a dark matter abundance of roughly the same size as what has been measured experimentally. This is such a surprising result that it has been named the "WIMP miracle".

In Chapter 4, I propose a new kind of WIMP model, in which DM is charged under the $SU(2)_w$ gauge group and also charged under a non-Abelian hidden $SU(N)$ gauge group. I study the case in which this hidden $SU(N)$ is unbroken and has a confinement scale that is much smaller than the current temperature of the universe. In this limit the dark gauge bosons associated with this gauge group correspond to new relativistic degrees of freedom in the universe. I first discuss how the effects of this extra gauge interactions change the sensitivity of different experiments searching for WIMP dark matter. Second, I discuss the imprints left by the dark gauge boson in the Cosmic Microwave Background and how this

constraints the model. I also explore the effects of the interactions between the dark gauge bosons and dark matter in the dark matter power spectrum. This chapter is based on a paper in preparation done in collaboration with M. Buen-Abad and M. Schmaltz.

2 Light axigluon explanation of the Tevatron $t\bar{t}$ asymmetry and multijet signals at the LHC

2.1 Introduction

The forward-backward asymmetry A_{FB} as measured in top quark pair production at the Tevatron continues to disagree with QCD predictions [19–22]. The asymmetry has been seen in events where only one of the top quarks decays leptonically and in events where both top and anti-top decay leptonically. Combining the single-lepton D0 analysis [10] of 5.4 fb^{-1} of data with CDF's single-lepton analysis [11] of 8.7 fb^{-1} and CDF's dilepton analysis [23] of 5.3 fb^{-1} we obtain[1] $A_{FB} = 0.185 \pm 0.037$ for the "unfolded" (parton level) asymmetry. This is 3.2 σ larger than the NLO QCD and electroweak prediction of $A_{FB} = 0.066$ obtained in [11] using POWHEG. Focusing on the dependence of the asymmetry on the invariant mass of the top pairs or their distribution in rapidity [25, 26] one obtains 3 σ deviations without the need to combine experiments. Altogether it appears very unlikely that the $t\bar{t}$ asymmetry at the Tevatron is due to statistical fluctuations. Standard Model predictions from different NLO event generators vary by amounts which are much smaller than the experimental errors, and NNLO as well as nonperturbative corrections are expected to be smaller yet. However, since the asymmetry first arises at NLO a reliable understanding of the theory errors requires a NNLO calculation which is currently in progress.

Axigluons [12, 20, 27–34] with a mass in the range from 100 to 400 GeV can explain the asymmetry. Such light axigluons appear to be the "last man standing"[2] of the large number of models (see e.g. [39–41] for an overview of the models and an extensive list of

[1] We used the method of [24] for combining the results and ignored correlations in systematic errors by adding statistic and systematic errors in quadrature.

[2] Recently, the authors of [35, 36] asserted that a complex Z' [37] coupling to up- and top-quarks can also explain the $t\bar{t}$ asymmetry and is consistent with all other constraints. The high energy tail of $t\bar{t}$ production predicted by such Z' models differs significantly from SM predictions, but it is consistent with current LHC measurements [38] which have large statistical uncertainties.

the original references). Other models have difficulty obtaining a large asymmetry at the Tevatron while remaining consistent with constraints from the total $t\bar{t}$ cross sections at the Tevatron and LHC, from the invariant mass spectrum of the $t\bar{t}$ cross sections, from bounds on single top and same-sign top production at the LHC, from the dijet cross section at the Tevatron, and from precision low-energy measurements such as atomic parity violation [42].

In this chapter we first review the current status of $t\bar{t}$ data in the context of a phenomenological light axigluon model (in Section 2.2). We find that the model fits all $t\bar{t}$ data very well. This encourages us to take the model more seriously and discuss constraints from other experiments. The most significant constraints come from pair production of axigluons at the LHC as we show in Section 2.3. Assuming that axigluons predominantly decay to quark-antiquark pairs one obtains a 4-jet final state with two dijet resonances of equal mass. This final state has been searched for by both ATLAS [2, 3] and CMS [4] and axigluons in the entire mass range from 100-400 GeV are ruled out. The beauty of this search is that it is independent of the strength and flavor structure of the axigluon coupling to fermions. It only assumes that axigluons are produced via QCD from initial state gluons (as required by QCD) and that they decay predominantly to quarks of any of the 5 light flavors (the searches did not require or exclude b-quarks). Axigluons of mass $> 2m_t$ could also predominantly decay to top quark pairs if the coupling to top quarks is enhanced. However the axigluon pair production cross section is so large (10s of pb for a 400 GeV axigluon at the 7 TeV LHC) that the resulting 4 top quark final state would have been seen, for example in CMS' same sign top search [43, 44].

Thus to save the light axigluon explanation of the $t\bar{t}$ asymmetry we must postulate that axigluons do not predominantly decay to dijets but instead decay to a new final state which has not been looked for or is very difficult to distinguish from backgrounds. Axigluons carry color, therefore the decay necessarily involves jets. In fact, it should involve only jets because any other particles in the final state (leptons, photons, missing E_T) would make the signal too easy to detect. And since decays to dijets are ruled out by the above-mentioned searches we are led to consider models in which the axigluon decays to three or more jets.

This can only dominate over the dijet decays if axigluons first undergo a two-body decay to intermediate resonances which then further decay to the final jets. The existence of such intermediate resonances with large couplings to axigluons is not far-fetched in axigluon models with small couplings to quarks. In fact, to obtain these small couplings one must introduce additional vector-like quarks for the SM quarks to mix with, and in the limit where the SM quarks couple weakly to the axigluon the new quarks couple strongly. Thus light axigluon models naturally contain additional particles which can catalyze the axigluon decays to multi-jet final states. The details of the spectrum of the new particles are model dependent and it is interesting to look for the most important possibilities.

In Section 2.4 we define four consistent axigluon models which cover the most important axigluon decay topologies. We outline their multijet signatures and discuss current bounds. We find that there are several possibilities for a large multi-jet signal to be observed in the near future. To facilitate the study of our models we provide [45] MadGraph [46] implementations created with FeynRules [47].

2.2 Phenomenological light axigluon model and $t\bar{t}$ data

The relevant parameters of our phenomenological axigluon model for the $t\bar{t}$ asymmetry are the axigluon mass m_A and width Γ_A and the products of its couplings to the light quarks (g_V^q, g_A^q) and to the top quark (g_V^t, g_A^t). In the center of mass frame and at tree level, the partonic $q\overline{q} \to t\bar{t}$ differential cross section including the interference between gluon and axigluon is

$$\begin{aligned}\frac{d\sigma(q\overline{q}\to t\bar{t})}{d\cos\theta} =& \frac{\beta}{144\pi s}\left\{\left[g_s^4(1+c^2+\frac{4m_t^2}{s})\right] + \right.\\ & \frac{2s(s-m_A^2)}{(s-m_A^2)^2+m_A^2\Gamma_A^2}\left[g_V^q g_V^t g_s^2(1+c^2+\frac{4m_t^2}{s}) + 2g_A^q g_A^t g_s^2\, c\right] + \\ & \frac{s^2}{(s-m_A^2)^2+m_A^2\Gamma_A^2}\left[((g_V^q)^2+(g_A^q)^2)\{(g_V^t)^2(1+c^2+\frac{4m_t^2}{s})+\right.\\ & \left.\left.(g_A^t)^2(1+c^2-\frac{4m_t^2}{s})\}+ g_V^q g_A^q g_V^t g_A^t\, 8c\right]\right\}\end{aligned} \tag{2.1}$$

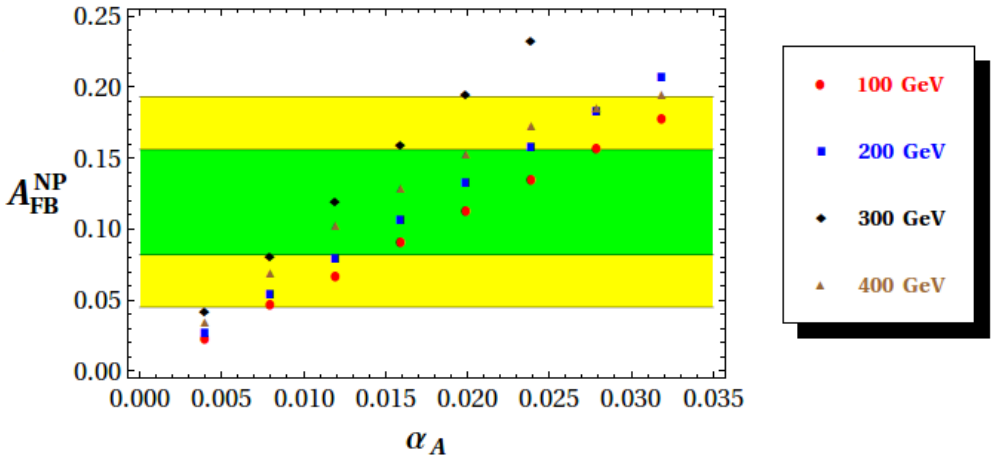

Figure 2.1: New Physics contribution to the parton-level forward-backward asymmetry A_{FB} at the Tevatron as a function of α_A for four different axigluon masses. Also shown are the one and two sigma bands obtained by combining the CDF and D0 measurements $A_{FB} = 0.185 \pm 0.037$ and subtracting a SM contribution of $A_{FB}^{SM} = 0.066$.

where $\beta \equiv \sqrt{1-4m_t^2/s}$. The asymmetric term proportional to $c \equiv \beta \cos\theta$ in the interference of the axigluon with the gluon (second line) requires non-vanishing axial couplings g_A^q, g_A^t. Vectorial couplings predominantly contribute to the symmetric part of the cross section and are strongly constrained by the good agreement of the measured cross section with SM predictions. We therefore choose purely axial couplings to both light and heavy quarks.[3] The axigluon width is important in determining the observability of the axigluon as a resonance in dijets at the Tevatron or UA1 and UA2. For $t\bar{t}$ production the width is relevant only when $m_A > 2m_t$ so that top quarks can be produced on resonance. Since we are interested in axigluon masses both below and above the $t\bar{t}$ threshold we choose a large width $\Gamma_A = 0.1 m_A$ for all of our reference points. The remaining parameters which determine the $t\bar{t}$ cross section and asymmetry at the Tevatron (and LHC) are then the product of the axial couplings to light and heavy quarks $\alpha_A = g_A^q g_A^t / 4\pi$ and the axigluon mass m_A.

[3]This restriction, $g_V^q = g_V^t = 0$, can be relaxed. Small vectorial couplings do not significantly change the multijet phenomenology which is the main focus of this chapter. Large vectorial couplings are disfavored by the good agreement of $t\bar{t}$ cross section shape with SM predictions as well as precision fits [42, 48].

In Figure 2.1 we show the predicted New Physics (NP) contribution to the $t\bar{t}$ asymmetry A_{FB}^{NP} at the Tevatron as a function of α_A for 4 representative axigluon masses $m_A = 100, 200, 300, 400$ GeV. The asymmetry is linear in α_A as long as $A_{FB}^{NP} \lesssim 15\%$, and large asymmetries can be obtained for moderate values of the couplings. A good fit (1 sigma) to the Tevatron data requires a NP contribution to the asymmetry between 8 and 16%. The asymmetry was calculated using MadGraph/MadEvent 5, as were all further calculations in the remainder of the chapter unless otherwise stated.

At the LHC $t\bar{t}$ production exhibits a small forward-central asymmetry, usually called "charge asymmetry" A_C. In the axigluon model A_{FB}^{NP} at the Tevatron and A_C^{NP} at the LHC are linear in α_A and therefore the predictions for the two asymmetries are also linearly related for small enough α_A. Figure 2.2 shows this correlation for four different axigluon masses. Also shown are lines indicating the boundaries of the 1σ preferred values for the asymmetries as measured at the Tevatron and LHC. For the LHC number we combined the CMS single-lepton measurement (with 4.9 fb^{-1}) [1] and the combined single-lepton (1.04 fb^{-1}) plus dilepton (4.71 fb^{-1}) result from ATLAS [49]. The colored areas correspond to the 68% and 95% preferred regions from our fit to the combined LHC and Tevatron measurements. The plot shows that axigluons with any mass in the range considered are consistent with asymmetry data at the 1σ level for appropriately chosen α_A.

For further comparison with other data we choose four reference axigluon models with masses 100, 200, 300, 400 GeV and choose axigluon couplings α_A (see Table 2.1) which produce 10% asymmetry from NP at the Tevatron. These models can now be tested against other $t\bar{t}$ data from the Tevatron and LHC. Columns 4 and 5 of the Table show the NP contributions to the $t\bar{t}$ cross section at the Tevatron and the LHC respectively. In all cases, the new contributions to the cross sections are much smaller than the experimental uncertainties of the cross section measurements of about ± 0.5 pb for the Tevatron [50, 51] and ± 5 pb for the LHC [52, 53]. Note that since our axigluon is light, the cross section enhancement is almost universal over the full range of $t\bar{t}$ invariant masses so that the shape of the cross section $d\sigma/dM_{t\bar{t}}$ does not give interesting constraints on the model.

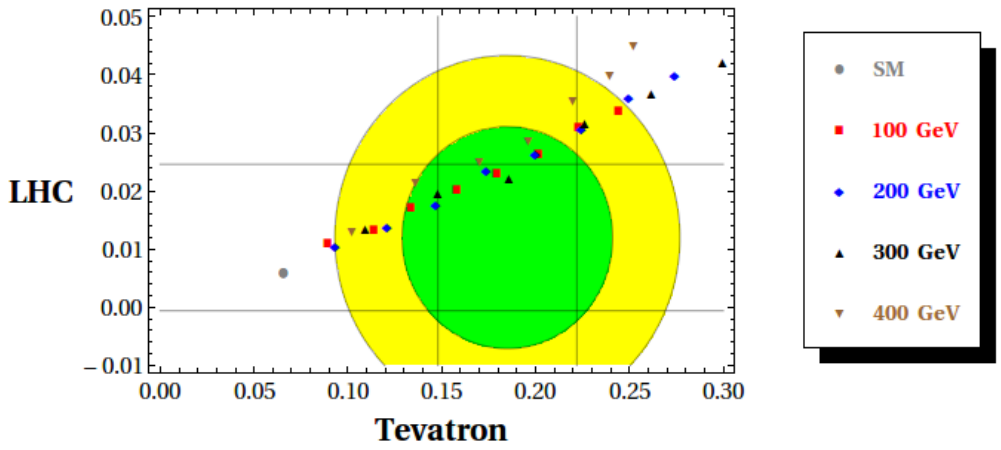

Figure 2.2: The LHC charge asymmetry and the Tevatron forward-backward asymmetry predicted in four axigluon models. The vertical and horizontal lines correspond to the the 1 σ boundaries of the experimentally preferred asymmetries for the Tevatron and LHC (see text). The shaded regions are preferred at 68% (green) and 95% (yellow) confidence level in a fit to the combined Tevatron and LHC measurements.

In order to increase its discriminating power, CMS also measured the charge asymmetry binned by the rapidity of the $t\bar{t}$ center of mass $|y_{t\bar{t}}|$. In Figure 2.3 we show the prediction for this differential asymmetry due to a 200 GeV axigluon added to the NLO Standard Model contribution compared with the experimental result [1]. There is a substantial increase in the predicted asymmetry for high $|y_{t\bar{t}}|$ which can be understood from the higher percentile of $q\bar{q}$ initial states in this kinematical region. The error bars are still too large to conclude anything definite, but given the large difference between the central value of the experimental result and the prediction, the charge asymmetry at high $y_{t\bar{t}}$ will become a very interesting discriminator [54–56] for our model in the future.

Finally, two additional independent $t\bar{t}$ physics observables which are sensitive to NP are two distinct FB asymmetries of the leptons produced in top decays. The FB asymmetry of leptons from events with large $t\bar{t}$ invariant mass is sensitive to the chirality of the produced top quarks [57], whereas the FB asymmetry of leptons from $t\bar{t}$ pairs produced near threshold is sensitive to NP with chiral couplings to the initial quarks in the colliding protons [58].

m_A/GeV	α_A	A_C^{NP}	$\sigma_{\rm Tev}^{NP}$/pb	$\sigma_{\rm LHC}^{NP}$/pb
100	0.018	0.016	0.06	0.2
200	0.015	0.016	0.05	0.2
300	0.010	0.016	0.04	0.2
400	0.012	0.018	0.37	1.4

Table 2.1: Axigluon coupling strength and NP contributions to top physics in four axigluon models. Each model produces a NP contribution to the $t\bar{t}$ asymmetry of 10% at the Tevatron. The Table gives the NP contribution to the LHC charge asymmetry, Tevatron $t\bar{t}$ cross section and LHC $t\bar{t}$ cross section.

The light axigluon model is in good agreement with the Tevatron data for both [11, 26].

2.3 Constraints from axigluon pair production at the LHC

In this Section we consider recent constraints from ATLAS and CMS which looked for pair-production of heavy resonances with subsequent decays to pairs of dijets. As we will see, these searches are very powerful in the case of the axigluon because the axigluon pair production cross section is enormous. It is enhanced by color and spin factors and is significantly larger than—for example—the pair production cross section of squarks, quarks, or even gluinos of the same mass. The cross section is largely model independent because it is dominated by gluon-gluon scattering $gg \to AA$ (see Fig. 2.5) which is uniquely fixed by gauge invariance and unitarity.[4]

The Lagrangian describing the relevant couplings of the axigluon to gluons is

$$\mathcal{L} = -\frac{1}{2}\mathrm{tr}\left(D_\mu A_\nu - D_\nu A_\mu\right)^2 + m_A^2 \mathrm{tr}\left(A_\mu A^\mu\right) + i\chi\ g_s\ \mathrm{tr}\left(G^{\mu\nu}[A_\mu, A_\nu]\right), \tag{2.2}$$

where $D_\mu A_\nu = \partial_\mu A_\nu - i g_s [G_\mu, A_\nu]$, A_μ is the axigluon field, g_s the strong coupling constant, G_μ the gluon and $G_{\mu\nu}$ is the gluon field strength. In addition, there can be three- and four-axigluon couplings which are not needed for axigluon pair production from gluon-gluon

[4] In addition to initial state gluons, there is also a contribution from quark anti-quark collisions (see Figure 2.6). However the latter is much smaller for all but the largest axigluon masses and we will ignore this process for the discussion in this Section.

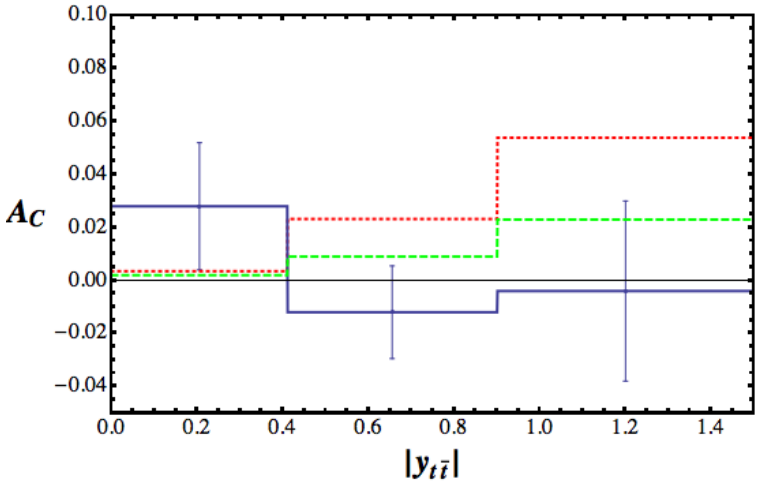

Figure 2.3: Differential charge asymmetry at the LHC as a function of the $t\bar{t}$ center of mass rapidity (data with 1 σ errors taken from [1]). The green dashed line corresponds to the QCD prediction at NLO, and the red dotted line is our prediction including the contribution of the 200 GeV axigluon from Table 2.1.

collisions. Renormalizable couplings with two gluons and a single axigluon are forbidden by $SU(3)_{color}$ gauge invariance. Loops of heavy particles can generate such couplings contained in dimension 6 operators. They are suppressed by a loop factor and heavy masses and we will neglect them.

Notice that beside the usual kinetic term for a colored vector field and the axigluon mass in Eq. 2.2, there is another renormalizable operator coupling gluons and axigluons given by the third term. Gauge invariance under ordinary color allows an arbitrary value for its coefficient χ, however unitarity of axigluon pair production amplitudes requires $\chi = 1$ [59]. To understand this, note that the calculation of the amplitude for production of massive vector bosons involves terms which grow with the scattering energy. In a consistent unitary theory these terms cancel due to the underlying spontaneously broken gauge invariance. This cancellation requires the coefficient $\chi = 1$. The presence of the χ-term can also be seen very easily in a weakly coupled UV completion of the axigluon model with the gauge symmetry breaking pattern $SU(3)_1 \times SU(3)_2 \to SU(3)_{color}$. Here the χ-term simply arises from rewriting the gauge boson kinetic terms of the mass eigenstates. More generally,

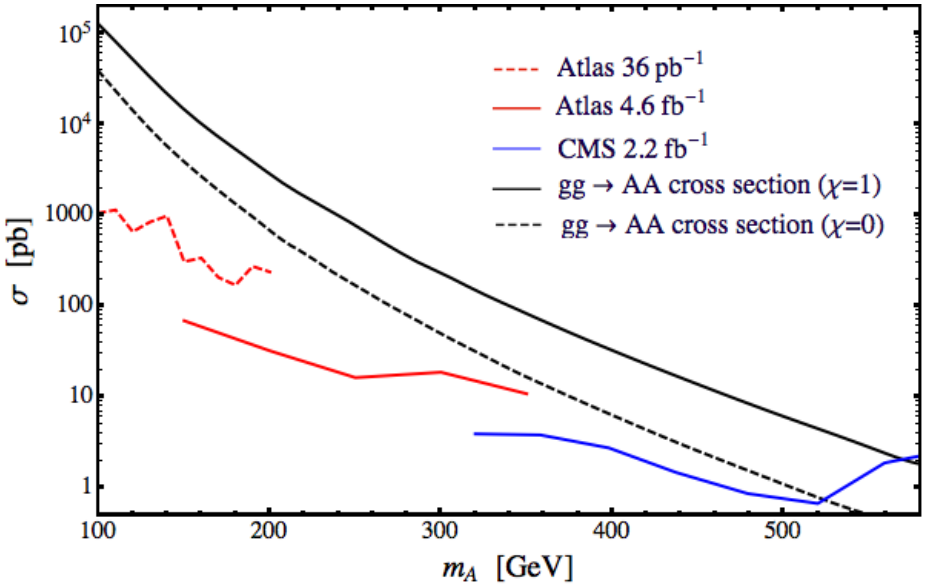

Figure 2.4: Axigluon pair production cross section from gluon initial states at the 7 TeV LHC as a function of the axigluon mass for $\chi = 1$ (solid) and $\chi = 0$ (dashed). Also shown are the upper bounds on this cross section obtained by ATLAS [2, 3] and CMS [4] which apply if axigluons decay with 100% branching fraction to dijets. The latter has been unfolded by comparing the cross-section times acceptance for coloron (axigluon) pair production presented in the analysis with our axigluon pair production cross-section calculated with MadGraph/MadEvent 5.

deviations from $\chi = 1$ are consistent with unitarity if they arise at the loop level or in the presence of additional massive colored particles contributing to the $gg \to AA$ process. We discuss the constraints imposed by unitarity on consistent axigluon models in Appendix C. For the remainder of the chapter we will use $\chi = 1$ for our plots.

Interestingly, while the χ-term suppresses the unphysical growth of scattering amplitudes in the UV, it enhances the amplitude near threshold where most of the cross section lies. Thus the total axigluon pair production cross section at the LHC is considerably enhanced by the χ-term as can be seen in Figure 2.4. This cross section is very large. For comparison, the cross section for axigluon pairs is only about factor of 5 below the total QCD dijet cross section (with a cut on jet p_T equal to m_A).

Also shown in Figure 2.4 are bounds on the axigluon pair production cross section from

three analyses at ATLAS and CMS. The bounds apply only to the case where the axigluon decays predominantly to dijets. The two ATLAS analyses focus on events with 4 hard jets and form the invariant masses of all possible combinations of jet pairs. Keeping only events in which the invariant masses of the two pairs of dijets are similar to each other one can enhance signal over background sufficiently. The 2010 ATLAS [2] analysis with 36 pb^{-1} takes advantage of the low instantaneous luminosity and low jet p_T triggers of the 2010 LHC run to search for light dijet resonances in the mass range from 100 to 200 GeV. The recent analysis of 4.6 fb^{-1} of data from 2011 [3] uses a similar technique with higher jet thresholds. It is sensitive to axigluon masses from 150 GeV to 350 GeV. Finally, the CMS analysis [4] looked for pair-produced dijet resonances in events with 4 hard jets ($E_T > 150$ GeV) and employed a "diagonal cut" [60] in order to enhance signal to background. The CMS analysis is sensitive to axigluon masses from 320 GeV to 580 GeV. Each of the three analyses excluded cross sections well below the axigluon one, and combining limits from all three analyses covers the axigluon mass range from 100 GeV to 580 GeV. Thus the simplest version of the light axigluon model with no new light particles below the axigluon mass is ruled out even when allowing for flavor non-universal axigluon couplings to quarks.

In the next Section we will discuss how these constraints can be evaded by opening up new axigluon decay channels with large branching fractions into multiple jets. This suppresses the branching fraction to dijets and creates new possibilities for discovering the axigluon in multijet resonance searches.

For completeness we now list other constraints on axigluon models which are independent of the above mentioned dijet resonance pair searches. However we emphasize that the dijet resonance pair searches alone are sufficient to rule out axigluons decaying to dijets.

- *Dijets:* Axigluons can be singly produced as an s-channel resonance decaying into quark-antiquark pairs. If the axigluon is sufficiently narrow it would lead to a clearly visible resonance in the dijet invariant mass spectrum. Assuming that there are no new decay channels for the axigluon, and assuming flavor-universal couplings to quarks the axigluon width $\Gamma_A = 5/(24\pi) g_A^2 m_A$ is negligible compared with experimental

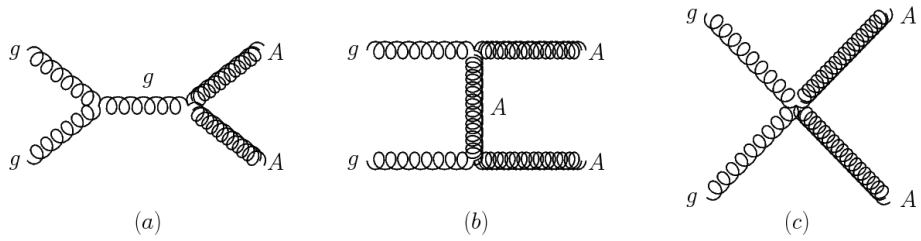

Figure 2.5: Diagrams contributing to axigluon pair production from initial state gluons: (a) gluon s-channel, (b) axigluon t-channel, (c) 4-point interaction.

resolution. Then the dijet searches by UA2 [61] and CDF [62] rule out axigluons with the necessary couplings to explain the $t\bar{t}$ asymmetry for all masses from 140 to 400 GeV. The dijet bounds can be evaded by reducing the couplings to first generation quarks and increasing the coupling to top quarks. We discuss dijet bounds in more detail in Appendix B.

- *Precision low energy measurements:* Axigluon couplings to quarks are also constrained by loop corrections to the Z coupling to quarks. These constraints are only significant for the smallest axigluon masses near 100 GeV [48]. Another potential constraint [42] derives from axigluon loop corrections to the Z coupling to quarks as measured in atomic parity violation. The couplings in our model are too small to give a significant effect.

- *Decays to b-quarks:* In the case of flavor non-universal axigluon couplings one might expect enhanced branching fractions to bottom quarks. CDF [63] has performed a search for a similar final state motivated by Higgs production in association with additional b-quarks. Assuming 100% branching fraction of axigluons to b quark pairs we find that the CDF study can be used to rule out masses up to 250 GeV.

2.4 New axigluon decay channels and multijets

In this Section we explore the possibility that the axigluon is broad because it has new decay channels with large partial widths. The cross section for pair production of axigluons

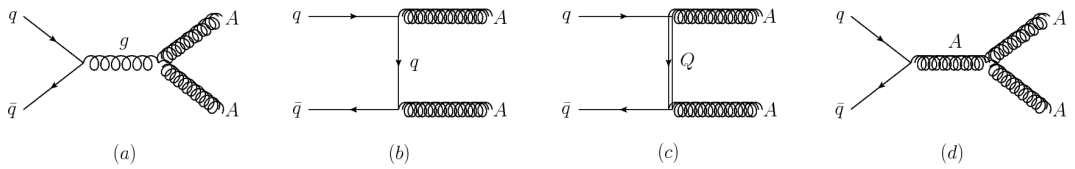

Figure 2.6: Diagrams contributing to axigluon pair production from a $q\bar{q}$ initial state: (a) gluon s-channel, (b) SM quark t-channel, (c) heavy quark t-channel, and (d) axigluon s-channel. All four diagrams have to be included with appropriately chosen axigluon couplings to preserve unitarity.

of mass m_A is only about an order of magnitude smaller than the huge QCD dijet cross section with jet transverse momenta $p_T > m_A$. Therefore these new decay channels have to be very difficult to detect or buried in QCD background to not have been ruled out already. This eliminates significant branching fractions to final states with leptons, photons or missing energy, and leaves decays to jets as the only realistic possibility. Figure 2.7 shows the cross section for axigluon pair production at the LHC with 8 TeV center of mass energy. It is dominated by the model independent $gg \to AA$ process, with the $q\overline{q}$ initiated process contributing only about 10%. If the $q\overline{q} \to AA$ process is included in event generations care must be taken to employ a consistent unitary model including all diagrams in Figure 2.6 (see Appendix C). For all axigluon masses between 100 and 400 GeV the cross section at the LHC is very large, producing $10^9 - 10^6$ events in the 2012 run. Thus if the signal can be isolated from QCD backgrounds the axigluon should be observable in multijets.

In the previous section we discussed axigluon decays to dijets and showed that axigluons which decay predominantly to dijets are ruled out over the entire mass range of interest. Here we focus on axigluons which decay preferentially to 3, 4, or 6 jets, giving events with 6-12 jets from axigluon pair production. Discovering or ruling out the axigluon is a matter of systematically eliminating the possible decay topologies. To this end we define four "simplified models" intended to study the four most "reasonable" decay topologies. The models are distinguished by different axigluon decay topologies which result from different intermediate particles through which the decay can proceed. We define the couplings of

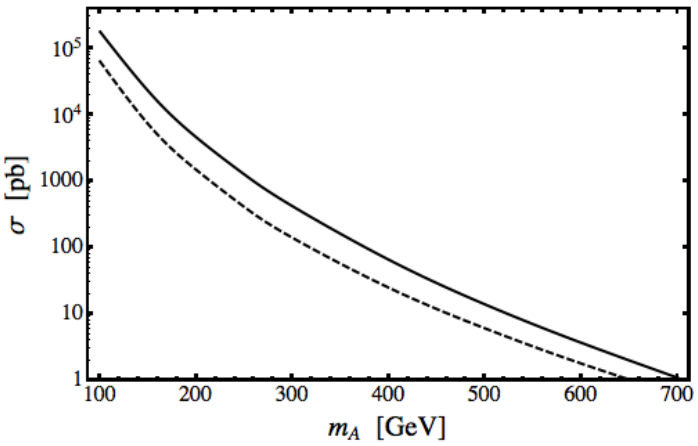

Figure 2.7: Axigluon pair production cross section at the 8 TeV LHC. Shown is the cross section with $\chi = 1$ (solid) and $\chi = 0$ (dashed). In both cases the cross section is dominated by the process $gg \to AA$ but includes the smaller $q\overline{q} \to AA$. The cross sections have been computed in the parity symmetric model of Appendix A with heavy quark masses set to 150 GeV, $g_A = 0$ and $g_{mixed} = g_s$.

the new particles and the axigluon as coefficients in an effective Lagrangian. Finally, we discuss collider signatures of each model and point out where existing searches already limit the allowed parameter space. For simplicity and for ease of comparison we assume 100% branching ratios to the selected final states. MadGraph implementations for each of the models are provided here [45]. UV-complete models which serve as explicit examples for the scenarios described here and demonstrate their consistency are presented in Appendix A.

Finally, before we discuss the models and the signatures of pair production of axigluons at the LHC we comment on single production of axigluons at the Tevatron via $q\overline{q} \to A$. If the axigluon predominantly decays to 3, 4 or 6 jets as postulated here one should also be able to see it as a resonance in 3, 4, or 6 jet events at the Tevatron. While a simple multi-jet resonance search is straightforward (one looks for a resonance in the total invariant mass spectrum of multijet events) we are not aware of any public results [5] except for a

[5]The dijet search from CDF [62] includes multijet events in the data because the analysis does not veto additional jets. However only the two leading jets are used to form the invariant mass which leads to

preliminary analysis from D0 [64] using 0.7 fb^{-1} and focusing on resonances above 400 GeV. For the case of flavor-universal axigluon couplings to quarks we expect that if any such resonance searches were performed at the Tevatron they could rule out axigluons in all of our models, at least for the heavier masses that we consider. For the lightest masses of order 100 GeV the jet-p_T thresholds at the Tevatron may already be too high. We urge that such multijet resonance searches at the Tevatron will be carried out and published as they would lead to strong limits. However, by allowing non-universal couplings it is possible to reduce the coupling to light quarks and reduce the single axigluon cross section by as much as two orders of magnitude. This would allow the multijet resonance to hide in the QCD background.

In the following, we return to discussing pair production at the LHC (and Tevatron). It is much more difficult to identify the resonances in pair production due to combinatoric backgrounds. However pair production has the big advantage that the cross section is model independent with no parameters which can be tuned to suppress it.

Scenario A, eight jets with scalar intermediate resonances

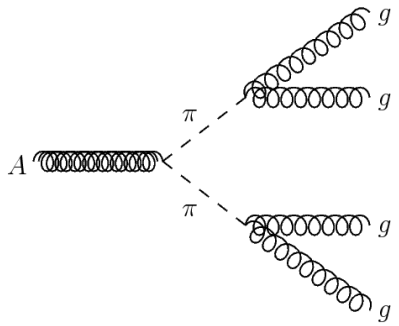

Figure 2.8: Axigluon decay to two scalar (or pseudoscalar) color-octets with subsequent decay to four gluons.

In this scenario there is a color-octet of scalars $\pi = \pi^a T^a$ with masses $m_\pi < m_A/2$ with strong couplings to axigluons so that axigluons decay predominantly to pairs of these

significant smearing and reduction of the reconstructed masses, and no significant bounds can be obtained.

scalars. The π^a further decay to pairs of gluons. Thus axigluon pair production leads to final states with eight jets with the resonance structure shown in Figure 2.8. This model is nice in that it has a simple signature and it is easy to construct consistent models with the necessary couplings. A drawback is that the introduction of the color-octet scalars is ad hoc. The scalars of this model can also be searched for directly through QCD pair production with subsequent decay to 4 jets. Existing searches do not exclude masses below 100 GeV down to 10s of GeV if the scalar carries no electroweak quantum numbers and has only small couplings to quarks. Above 100 GeV only a small mass window around 140 GeV is allowed by the aforementioned ATLAS search [3].

Lagrangian

The Lagrangian describing the couplings of the scalar to axigluons A^a_μ and gluons G^a_μ is

$$\mathcal{L} = \frac{1}{2}\left(D^\mu\pi\right)^a\left(D_\mu\pi\right)^a + \lambda_A f^{abc} A^a_\mu \pi^b (D^\mu\pi)^c + \frac{g_s^2}{16\pi^2\Lambda}\mathrm{tr}\left(\pi\, G_{\mu\nu}G^{\mu\nu}\right), \tag{2.3}$$

where $(D_\mu\pi)^a = \partial_\mu\pi^a + g_s f^{abc} G^b_\mu \pi^c$ and $G_{\mu\nu} = \partial_\mu G_\nu - \partial_\nu G_\mu - i g_s [G_\mu, G_\nu]$ is the gluon field strength. The coupling constant λ_A must be at least of order 1 so that axigluon decay to scalars dominates over decay to quarks. The mass parameter Λ determines the scalars' decay width to gluons. In a UV completion it may correspond to the mass of new vector-like fermions, and the operator $\mathrm{tr}\left(\pi\, G_{\mu\nu}G^{\mu\nu}\right)$ is generated when integrating out these fermions.[6]

Phenomenology

How the multi-jet signal materializes depends on the relative mass of the axigluon and the scalar. In order for the axigluon decays to scalars to dominate over decay to quarks the scalar must be significantly lighter than half the axigluon mass. On the other hand, for $m_\pi \lesssim m_A/8$ the opening angle between the two gluon jets from each scalar decay becomes so small that the jets merge. Then the 8 gluon final state would be observed as 4 jets and

[6] Several modifications of this simple model are possible. Instead of the scalar we could have a pseudoscalar which couples to gluons as $\mathrm{tr}\left(\pi\, G_{\mu\nu}\widetilde{G}^{\mu\nu}\right)$. The scalar or pseudoscalar may also decay to quark anti-quark pairs, and one would expect the heaviest accessible quarks, the b-quarks, to dominate.

the CMS and ATLAS bounds in Figure 2.4 apply. Thus for this model to be viable scalar masses must lie roughly between 1/8 and 1/2 of m_A.

Given the large cross section there are several options for probing this model. Perhaps the most straightforward is to look for a threshold feature at twice the axigluon mass in final states with large numbers of jets. An alternative would be to make use of the resonance structure of the events and identify resonances in 2 or 4 jet invariant mass distributions corresponding to the scalars and axigluons.

A search of the former kind which could potentially be sensitive to axigluon pair production is the CMS Black hole search [65]. Here one looks for an enhanced rate of multi-jet final states at large invariant masses or large S_T. The publicly available analysis is not sensitive to axigluon pair production near threshold for the axigluon masses of interest because of high jet-p_T thresholds and a focus on very large $S_T > 1.8$ TeV. However one might still see an enhancement of the cross section at the highest energies due to the large tail of the axigluon pair production cross section. This is more difficult than looking for the threshold bump because it requires a theoretical prediction of the QCD background. Another issue is that the number of jets observed depends on the relative size of jet-p_T cuts, the axigluon and scalar masses and typically some jets are lost. On the other hand, the number of jets can also exceed 8 due to the large amount of QCD radiation expected from an 8 gluon final state.

The alternative search strategy would be to look for invariant mass bumps in multijet events. In principle one can try to identify both the mass of the axigluon as a 4 jet resonance and the mass of the scalar as a 2 jet resonance.[7] The 2 jet resonance is easier to reconstruct, especially if the scalars are boosted so that the two gluon jets from their decay are near each other. For example, if $m_\pi \lesssim m_A/4$, then one might define broad jets ($R \sim 1$) to capture the two gluon jets from each scalar decay in one broad jet. Then jet-substructure techniques [67–76] could be used to look for subjets within the broad jets which combine into a resonance

[7] Simultaneous with the posting [13], CMS released a preliminary analysis searching for 8jet finals states with this topology which is sensitive to (and rules out) axigluon masses above 400 GeV [66]. Going to lower masses is more difficult due to trigger thresholds.

at m_π. The axigluon resonance is more difficult to reconstruct in general because of large combinatoric backgrounds. Axigluon bump hunting might be most promising in events where the axigluons are produced significantly above threshold so that the decay products of the two axigluons are boosted and do not overlap.

For previous phenomenological work on a very closely related model with explicit proposals for cuts to enhance the resonance signals see for example [59, 77].

Scenario B, 12 jet final state

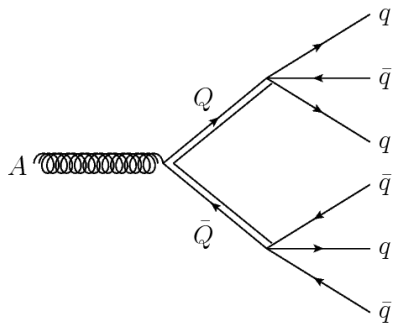

Figure 2.9: Axigluon decay to two heavy color-triplet fermions with subsequent decay to six quarks.

In this scenario we consider new fermions (heavy quarks) which transform as color triplets like the ordinary quarks. Axigluons are assumed to predominantly decay into pairs of these heavy quarks. The heavy quarks subsequently each decay to 3 light quarks via off-shell axigluons. Thus in this model pair production of axigluons leads to 12 jet final states as shown in Figure 2.9. This model is natural in the sense that heavy vector-like quarks are already required by unitarity in a renormalizable axigluon model (see Appendix A). Unitarity and bounds from LEP2 constrain the masses of these heavy quarks to lie between 100 GeV and approximately 1 TeV.[8] For definiteness, we assume that only one of the heavy quarks is lighter than 1/2 of the axigluon mass so that only this fermion is

[8]We discuss the relationship between heavy fermion masses and unitarity of the axigluon pair production cross section in Appendix C.

involved in axigluon decays. All other fermions are assumed to be near 1 TeV so that they are irrelevant to axigluon decays. Alternatively, one could have also chosen multiple heavy quarks to be light.

In principle there are constraints from direct pair production of the heavy quarks at the LHC with subsequent decay to six jet final states. However, the pair production cross section of the quarks is sufficiently small that even several flavors of such color-triplet fermions decaying to three jets are allowed by all searches [78, 79].

Lagrangian

Using two-component spinors for the fermions, the Lagrangian describing the couplings of the axigluon to the vector-like heavy quark $(D_H, \overline{D}_H)$ is

$$\mathcal{L} = \lambda_H A^a_\mu D^\dagger_H \sigma^\mu T^a D_H + \overline{\lambda}_H A^a_\mu \overline{D}^\dagger_H \sigma^\mu T^{a*} \overline{D}_H + (\lambda_{\rm mix} A^a_\mu D^\dagger_H \sigma^\mu T^a D_{SM} + h.c.)\,. \qquad (2.4)$$

Here D_{SM} is a right-handed down-type SM quark, D_H has the same quantum numbers as D_{SM} and has a mass with its vector partner, $M_{HQ}\, D_H \overline{D}_H$. Since we are only including a single heavy quark, the mixed coupling to D_{SM} necessarily breaks the SM flavor symmetries. Flavor constraints on the couplings of 1st and 2nd generation quarks are generally stronger than constraints on 3rd generation quarks. Therefore we chose the mixed coupling to only involve the right-handed bottom quark, i.e. $D_{SM} \equiv b_R$. Then axigluon decays give final states with at least two b-jets. In order to ensure that the axigluon predominantly decays to pairs of heavy quarks one of the couplings λ_H or $\overline{\lambda}_H$ has to be larger than g_s and also $\lambda_{mix} \ll \max[\lambda_H, \overline{\lambda}_H]$. Explicit expressions for $\lambda_H, \overline{\lambda}_H$, and λ_{mix} in terms of parameters of a UV-complete model are given in Appendix A (and utilized in our MadGraph implementation of the model). These expressions imply relations between the couplings which ensure unitary amplitudes.

Phenomenology

Axigluon pair production in this model leads to a final state with even larger jet multiplicity than the one described in Scenario A. Combinatoric backgrounds to reconstruction of any of

the resonances are therefore much larger. Thus any searches which focus on reconstructing axigluons or heavy fermions must rely on boosted events and possibly use jet substructure techniques.

On the other hand, since the axigluon pair-production cross section is much larger than the background QCD 12-jet cross section one might expect to see a bump in the measured cross section for very high multiplicity jets. A search of this kind would be similar in spirit to the CMS black hole search [65] but would have to use much lower p_T cuts. There is significant sensitivity to jet-p_T thresholds and the relative size of the axigluon and heavy quark masses, and in practice many of the jets may be lost due to cuts and jet merging.

Scenario C, 8 jets with fermionic intermediate resonances

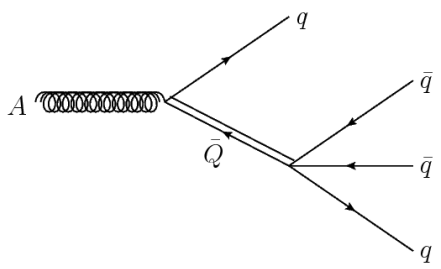

Figure 2.10: Axigluon decay to a heavy color-triplet fermion in association with a light quark giving rise to a 4 quark final state.

In this scenario the axigluon is assumed to decay to a SM quark in association with a heavy vector-like quark. This heavy quark further decays to three light quarks so that axigluon decays lead to 4 light quark jets in the final state as shown in Figure 2.10. In order to get a sufficiently large decay width to this final state we choose several such new heavy quarks. This scenario occurs naturally in renormalizable axigluon models in which the coupling of the axigluon to quarks is suppressed due to mixing with heavy quarks. In those models small axigluon couplings to SM quarks are correlated with large mixed couplings

λ_{mix} of the axigluon to one SM quark and one heavy quark (see Appendix A).

Lagrangian

Using two-component spinors for the fermions, the Lagrangian describing the mixed couplings of the axigluon to the vector-like heavy quarks and light quarks is

$$\mathcal{L} = \lambda^{U}_{\rm mix}\, A^{a}_{\mu} U^{\dagger}_{H} \sigma^{\mu} T^{a} U_{SM} + \lambda^{D}_{\rm mix}\, A^{a}_{\mu} D^{\dagger}_{H} \sigma^{\mu} T^{a} D_{SM} + h.c.\,. \tag{2.5}$$

Here U_{SM} and D_{SM} are right-handed up- and down-type SM quarks, U_H (D_H) has the same quantum numbers as U_{SM} (D_{SM}). The heavy quarks have masses with vector-like partners $\overline{U}_H, \overline{D}_H$, for example $M_{HQ}\, U_H \overline{U}_H$. Explicit expressions for $\lambda^{U/D}_{mix}$ in terms of parameters of a UV-complete model are given in Appendix A (and utilized in our MadGraph implementation of the model). These expressions imply relations between g_s, g_A and $\lambda^{U/D}_{mix}$ which ensure unitary amplitudes.

A few comments about the flavor structure of this scenario are in order. First, experimental searches for new heavy quarks with significant branching fractions to final states with W's and Z's rule out such new quarks with masses below 500 GeV. Mixing with third generation quarks generally introduces decays involving W's and Z's, and therefore we consider new quarks which only couple to 1st and 2nd generation quarks. This necessarily implies some level of flavor violation. Constraints from flavor physics further forbid large couplings to quark doublets. This is why we did not include couplings to quark doublets in the Lagrangian in Eq. 2.5. Introducing heavy quark singlets without corresponding heavy quark doublets breaks parity symmetry in the axigluon coupling to heavy fermions. In a complete model one would therefore expect the axigluon couplings to light quarks to not be purely axial without fine tuning.

To summarize, we consider two generations of degenerate heavy quarks, two of up-type U_H and two of down-type D_H and their vector-like partners. The couplings $\lambda^{U/D}_{mix}$ are chosen to preserve the flavor symmetries of the 1st and 2nd generation.

Phenomenology

Axigluon pair production in this model leads to a final state with eight light quark jets as in model A. Most of the discussion for model A also applies in this case. The main difference is that because of combinatoric backgrounds reconstruction of a three jet resonance is more difficult than the reconstruction of two jet resonances. The other difference is that in this model there can be a significant asymmetry between the typical p_T of the jets from the heavy fermion decays and the jet from the primary axigluon decay. This asymmetry depends on the relative mass of the axigluon and heavy fermions and contributes to the efficiency with which these events are picked up in searches similar to the black hole searches.

Scenario D, interpolating between 6 and 8 jet final states

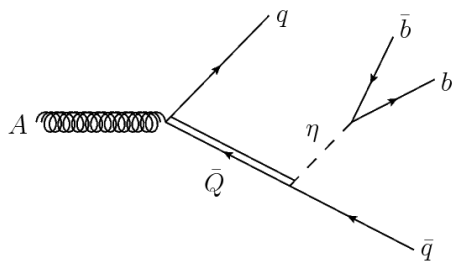

Figure 2.11: Axigluon decay to heavy color-triplet fermion in association with a light quark. The heavy quark subsequently decays to a SM quark and a light scalar which further decays to b-quarks.

This scenario is identical to scenario C except that there is an additional light color-singlet scalar particle η which participates in the heavy quark decay. Thus axigluons now decay through a small decay chain as shown in Figure 2.11. Light singlet scalars arise naturally in axigluon models as uneaten components of the field(s) that break the UV gauge symmetry down to QCD giving mass to the axigluon. In the simple case where $SU(3)_1 \times SU(3)_2$ is broken to the diagonal 8 Nambu-Goldstone bosons are eaten to give

a mass to the axigluon. However there is a 9th NGB, "axion", because the full global symmetry breaking structure is really $U(3)_1 \times U(3)_2$ broken to diagonal $U(3)$. This uneaten NGB is naturally light and can play the role of η. Its mass can be chosen arbitrarily by adding small explicit symmetry breaking interactions. We envision η masses in the range from 10 GeV to the axigluon mass for this scenario. In the axigluon models described in [12] the η is expected to have large mixed couplings with a SM quark and a heavy quark, so that heavy quarks preferentially decay into light quarks and η. In addition η also has a small coupling to two SM quarks which arises from mixing proportional to the SM quark masses. This coupling is largest for the third generation quarks and causes the scalar to decay almost exclusively to bottom quark pairs.

Lagrangian

The Lagrangian describing this model is the same as model C, plus a new piece describing the axion interactions,

$$\mathcal{L} \supset \frac{1}{2}(\partial\eta)^2 - \frac{1}{2}\mu_a^2\eta^2 + i\lambda_b\eta(b_L^\dagger b_R - b_R^\dagger b_L) + \left(\lambda_a\eta\overline{U}_H U_{SM} + \lambda_a\eta\overline{D}_H D_{SM} + h.c.\right). \quad (2.6)$$

In the equation above, μ_a is the axion's mass, λ_a is the coupling that controls the decay of the heavy quark to a quark and the scalar and λ_b the coupling that controls the decay of the axion to the SM bottom quarks. λ_b is not the SM bottom Yukawa coupling, but it is proportional to it because it is generated by mixing proportional to quark masses.

Phenomenology

In this scenario the axigluon decays to a heavy quark and a light quark as in model C. The heavy quark then decays to a quark and the axion, which in turn decays to two bottom quarks. Thus each axigluon decays to 2 light quarks and 2 b quarks as shown in Figure 2.11. The phenomenology of this model is interesting as it interpolates between final states with 6 to 8 jets. When the η mass is a sizeable fraction of the heavy quark mass all 8 jets are in principle observable as separate jets. However when the mass of η is closer to 10 GeV the b-quarks from η-decay become collimated and merge into a double-b jet. This double-b jet

is quite interesting. It contains substructure due to the presence of two b-quarks and it is very likely to be tagged as a b-jet because it contains 2 displaced vertices. Double-b jets are not unreasonable to occur in many models beyond the SM which contain light scalars and are an interesting signature to look for independent of the multi-jet final states we propose here.

How would one look for this model? In the case of large η masses, the phenomenology is very similar to the 8 jet finals states which we discussed before. One can focus on searching for bumps in di-dijet invariant masses or take advantage of the high jet multiplicity of the events as discussed in Scenario A. For the smallest η masses the model is already mostly ruled out by the 6 jet final state searches for R-parity violating gluino decays [78, 79]. If one takes the limit from these searches at face value there is only a small window in axigluon masses between 170-200 GeV (near the top mass) where this scenario is not ruled out. However the acceptance of the search to the axigluon decay signal depends on the mass of η. Thus this model motivates an interesting possible extension to the current 6-jet resonance searches for R-parity violating gluino decays.

3 Higgs mass naturalness and scale invariance in the UV

3.1 Introduction

The observation [5, 6] of a light Higgs boson with properties which are consistent with the Standard Model (SM) has motivated much reexamination of the notion of naturalness [80–82]. In theories of natural electroweak symmetry breaking the Standard Model is modified at high scales to incorporate a symmetry which protects the mass of the Higgs boson from sensitivity to high scales. Supersymmetry or the shift symmetries of Little Higgs theories require the introduction of "partner" particles which cancel the contributions to the Higgs mass from Standard Model particles. The cancellation between SM particles and partners occurs for each value of the loop momentum.

A qualitatively different proposal is to use conformal symmetry to protect the Higgs mass.[1] The idea is that if the Higgs scalar field were part of a conformal field theory (CFT), then its mass would be forbidden by scale invariance. Of course, the SM has particle masses and running couplings which break conformal symmetry. However, if conformal symmetry could be broken sufficiently "softly" such that the symmetry is restored at high energies, then the Higgs mass would still be protected from the largest radiative corrections which come from the highest energies.

The idea to use scale invariance to protect the Higgs mass was proposed long time ago in [16] and has recently received some attention [85–108]. In the recent literature, scale invariance of the classical Lagrangian is often invoked to argue the absence of large quantum corrections. This is misguided because only symmetries of the quantum theory constrain the form of possible counter terms. Thus to employ scale invariance for protecting the Higgs mass one has to show that all SM coupling constants approach fixed points when evolved

[1] Scale invariance is sufficient to protect the Higgs mass. It is believed that for unitary and causal $4d$ quantum field theories scale and Lorentz invariance imply conformal invariance [83, 84], therefore we do not distinguish between scale and conformal invariance in this chapter.

into the ultraviolet (UV) with the renormalization group.[2] An obvious problem is that in the SM both gravitational and hypercharge couplings grow at short distances. If unchecked, each coupling becomes non-perturbatively large at a characteristic scale in the UV, leading to very large conformal symmetry breaking near the Planck scale and the hypercharge Landau pole, respectively. Thus, at the least hypercharge and gravitational interactions must transition from their current evolution to the CFT behavior before the couplings become non-perturbatively large. If this transition involves ultra-heavy particles these particles can appear in virtual corrections, and it is well-known that loops of massive particles destabilize the Higgs mass. But what if there are no heavy particles at the transition scales? And are there constraints on the evolution of asymptotically free couplings like the QCD coupling which do not grow in the UV?

In this chapter we show that the Higgs mass is sensitive to any threshold scales in the UV, including scales which only arise from dimensional transmutation and are therefore hidden from Feynman diagram calculations at fixed loop order. Our argument relies on the fact that anomalous dimensions of operators which couple to the Higgs change as the threshold is crossed. Given this sensitivity of the Higgs mass to the threshold scale, it is clear that naturalness requires the transitions to happen at low scales (near the TeV scale for hypercharge and below $\sim (M_{\rm Weak} M_{\rm Planck})^{1/2}$ for gravity).

The proposal of a CFT in the UV requires us to think carefully about the notion of fine tuning. In the usual effective field theory picture we envision a cutoff beyond which the laws of physics are unknown (generally at or below the Planck scale), and counter terms at the cutoff encode contributions from unknown physics above the cutoff. A theory is then natural if the coefficients of operators in the effective theory below the cutoff are stable against quantum corrections in the effective theory.

It is important to distinguish between technically natural parameters like a chiral fermion mass which are protected by symmetries and parameters which are not protected by sym-

[2] A less ambitious proposal is to merge the non-gravitational couplings into a CFT between the weak and the Planck scale [109, 110] and assume that unspecified quantum gravitational dynamics sets the desired conformal boundary conditions at Planck scale. Our results apply to either case.

metries. For the chiral fermion, all contributions to the mass are proportional to chiral symmetry breaking. Therefore, the renormalized mass can be kept fixed by scaling chiral symmetry breaking to zero at the same time as taking the regulator to infinity. In contrast, a parameter which is not protected by symmetries receives additive contributions from renormalization. If these contributions are divergent then fine-tuning of the bare parameter against quantum corrections is required to keep the parameter finite as the regulator is taken to infinity. While such tuning is a mathematical possibility, it is unnatural unless it is enforced by a symmetry. Scale invariance can play the role of this symmetry, but since scale invariance is broken in the Standard Model one must ensure that scale invariance violation is soft, i.e. no new divergences are introduced by the couplings which break scale invariance. In the following sections, we explain this criterion with specific examples and show that the approach to the UV fixed point has to be sufficiently rapid so that conformal symmetry breaking does not enter the Higgs mass corrections from the UV. Only then is it natural to invoke UV scale invariance to cancel away the Higgs mass contributions from the UV. We find that deviations of the gauge couplings from their UV fixed point values must scale away as sufficiently large powers of distance at short distances. For example, the logarithmic approach to the free fixed point of the QCD coupling in the SM is too slow, and contributions to the Higgs mass due to the scale invariance violation from to the running QCD coupling persist to arbitrarily high energies. Thus, even the asymptotically free couplings of the SM must transition to different UV behaviors for the Higgs mass to be protected by scale invariance.

Given our results, it is clear that a successful implementation of "Higgs mass naturalness from scale invariance in the UV" requires major modifications of the Standard Model at the TeV scale. In particular, all gauge couplings must turn over and approach non-trivial fixed points near the TeV scale because free fixed points always lead to logarithmic running. We emphasize that our results apply irrespective of the choice of regulator. Dimensional regularization is often most convenient for calculations, but the apparent absence of power divergences in dimensional regularization does not remove sensitivity to high scales and

associated fine tuning.

In Section 3.2 we review the calculation of quantum corrections to the Higgs mass in perturbative theories and discuss the connection to scale invariance. In Section 3.3 we define toy models for field theories which transition between different fixed point behaviors in the UV and IR. We show explicitly that the Higgs mass is sensitive to the threshold scale in the anomalous dimensions which result from the differing UV and IR scalings. In Section 3.4 we show that dimensionless couplings which are asymptotically free lead to logarithmic breaking of scale invariance in anomalous dimensions. Hence in asymptotically free theories, scale invariance cannot protect the Higgs mass from large corrections in the UV. We conclude in Section 3.5.

3.2 Higgs mass sensitivity to the UV and scale invariance

Consider a toy SM with a Dirac fermion "top quark" t with a chiral coupling to a complex scalar "Higgs"

$$\mathcal{L} = -\lambda_t (h\,\bar{t} P_L t + h^\dagger\,\bar{t} P_R t)\ . \tag{3.1}$$

Assuming a non-vanishing fermion mass,[3] m_t, the usual top quark contribution to the Higgs mass (Figure 3.1) is

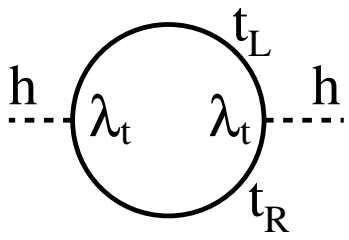

Figure 3.1: Top quark loop contribution to the Higgs mass.

[3]Or equivalently expanding about non-zero h expectation value. We also introduce the renormalization scale μ to account for the change in dimension of the coupling λ_t in d dimensions. The scale is arbitrary and will not be very important for our discussion.

$$\begin{aligned}
\delta m_h^2 =& -iN_c\lambda_t^2\mu^{4-d}\int\frac{d^dp}{(2\pi)^d}Tr\left[P_L\frac{\not{p}+m_t}{p^2-m_t^2+i\epsilon}P_R\frac{\not{p}+m_t}{p^2-m_t^2+i\epsilon}\right]\\
=& -2iN_c\lambda_t^2\mu^{4-d}\int\frac{d^dp}{(2\pi)^d}\frac{p^2}{(p^2-m_t^2+i\epsilon)^2}\\
=& -\frac{N_c\lambda_t^2}{8\pi^2}m_t^2\left(\frac{4\pi\mu^2}{m_t^2}\right)^{\frac{4-d}{2}}\frac{d}{2}\Gamma(1-\frac{d}{2})\\
=&\frac{N_c\lambda_t^2}{4\pi^2}m_t^2\left(\frac{1}{\epsilon}-\gamma-\log\frac{m_t^2}{4\pi\mu^2}+\frac{1}{2}\right)
\end{aligned}\tag{3.2}$$

near $d = 4 - 2\epsilon$. This becomes $\delta m_h^2 = -m_t^2 N_c\lambda_t^2/(4\pi^2)(\log[m_t^2/\mu^2] - \frac{1}{2})$ after modified minimal subtraction $\overline{\text{MS}}$ of the UV divergence. Famously, there is no quadratic divergence and the correction is proportional to a finite scale, the top quark mass m_t.

However, the answer is regulator dependent. In fact, there are additive contributions from any finite momentum shell above m_t which grow with momentum squared. If we had used a momentum cutoff Λ these contributions would have been more explicit, and we would have had to remove the quadratic divergence "by hand" to obtain a finite answer. In absence of a symmetry, the remaining Higgs mass is arbitrary because the counter term which cancels the divergence is only determined up to an additive constant. And since the contributions from short distances grow without bound, any finite Higgs mass requires fine tuning the counter term. Dimensional regularization with $\overline{\text{MS}}$ is misleading in this case because it does the tuning automatically, but it does not change the fact that there is sensitivity to high scales and additional finite pieces could be added to the counter terms.

To decide whether the fine-tuning in this example is intrinsic to the theory or just an artifact of a poorly chosen regulator requires careful consideration of the symmetries. In particular, we could imagine that our top-Higgs system is embedded in a larger theory which is conformal in the UV. The conformal symmetry is broken by the top mass, but since the mass is a relevant operator one might try to argue that conformal symmetry is restored in the UV. If that were true, a vanishing Higgs mass in the UV would correspond to an enhanced symmetry point. Then a Higgs mass counter term which cancels all contributions from the top loop above m_t would be perfectly natural. Unfortunately, this argument is not correct and even this simple example is more subtle.

To understand the subtlety, consider first the same calculation as above with a vanishing top mass. Then our toy theory really is conformal and the above argument applies. In dimensional regularization we would compute

$$\delta m_h^2 \propto \int \frac{d^d p}{(2\pi)^d} \frac{1}{p^2} = 0 \ . \tag{3.3}$$

The vanishing result is a consequence of scale invariance of the theory. The same result could have also been obtained with a momentum cutoff Λ as a regulator. This regulator clearly violates conformal invariance, and the integral would have been proportional to Λ^2. However, the underlying scale invariance of the theory requires us to choose the counter term such as to cancel this contribution exactly.

We are now ready to consider the effects of conformal symmetry breaking from the top mass. This adds a new logarithmic divergence proportional to $m_t^2 \log(\Lambda^2/m_t^2)$. The explicit m_t-dependence of the divergence makes it manifest that conformal invariance is not restored in the UV. There contributions to the Higgs mass grow without bound as the cutoff is taken to infinity, and canceling them with a counter term to obtain a finite Higgs mass constitutes fine-tuning. In particular, for exponentially large cutoffs Λ there is no sense in which a Higgs mass near the top quark mass is preferred by the symmetries.

How does this compare with the innocuous looking result obtained in dimensional regularization with $\overline{\text{MS}}$? The dimensional regularization answer before inclusion of the counter term does contain the divergence in the form of the $1/\epsilon$ term. After subtraction, the renormalized mass is finite because the contributions from the UV have already been fine-tuned away. We can still see them in the dependence of δm_h^2 on μ. Taking μ exponentially larger than m_t we see that the running $\overline{\text{MS}}$ Higgs mass at large μ becomes much larger than m_t. The small value at $\mu \sim m_t$ is a result of fine-tuning the UV Higgs mass parameter in order to obtain a small mass in the IR.

In the following, we will find it convenient to calculate the Higgs mass contribution in position space

$$\delta m_h^2 = i(-i\lambda_t)^2 \mu^{4-d} \int d^d x \langle 0|T\, \mathcal{O}^\dagger(x)\mathcal{O}(0)|0\rangle. \tag{3.4}$$

This reproduces the momentum space result after plugging in the (normal ordered) operator $\bar{t}P_L t$ for $\mathcal{O}$, contracting fields with propagators, and integrating over x

$$\begin{aligned} & \int d^d x \, \langle 0|T\,(\bar{t}P_R t)(x)\,(\bar{t}P_L t)(0)|0\rangle \\ = \;& -N_c \int d^d x \; Tr\left[\int \frac{d^d p}{(2\pi)^d} e^{ipx} P_L \frac{i(\not{p}+m_t)}{p^2-m_t^2+i\epsilon} P_R \int \frac{d^d q}{(2\pi)^d} e^{-iqx} \frac{i(\not{q}+m_t)}{q^2-m_t^2+i\epsilon}\right] \\ = \;& 2N_c \int \frac{d^d p}{(2\pi)^d} \frac{p^2}{(p^2-m_t^2+i\epsilon)^2} \; . \end{aligned} \tag{3.5}$$

How would the position space computation be modified if the the Higgs coupled to an interacting CFT? To have an example theory to consider, we construct a class of perturbative models similar to those proposed by Banks and Zaks [111]. Consider QCD with a large number of colors N_c and the number of flavors chosen such that the gauge coupling has a weakly-coupled IR-stable fixed point. Perturb the theory by coupling a single complex scalar "Higgs" with a flavor-universal Yukawa coupling to all quarks of the CFT as in (3.1). The coupling is a relevant perturbation because $\mathcal{O} = \bar{t}P_L t$ has negative anomalous dimension. The one-loop beta function for the Yukawa coupling also has an IR stable fixed point. Setting the gauge and Yukawa couplings to their fixed point values $g = g^*$ and $\lambda_t = \lambda_t^*$ in the UV, this theory is conformal at all scales.[4] This defines an interacting CFT with a negative anomalous dimension $\gamma_{\mathcal{O}}$ for $\mathcal{O}$.

The two point function of $\mathcal{O}$ in (3.4) is determined by conformal invariance

$$\langle 0|T\mathcal{O}^\dagger(x)\mathcal{O}(0)|0\rangle = C\left(\frac{1}{-x^2+i\epsilon}\right)^{d-1+\gamma_{\mathcal{O}}}, \tag{3.6}$$

where $x^2 = t^2 - \vec{x}^2$. The constant C depends on the normalization of the operator which we choose such that $C = 1$. Now the computation of the Higgs mass in the CFT is simple. To lowest order in λ_t, we obtain

$$\delta m_h^2 = -i\lambda_t^2 \mu^{4-d} \int d^d x \left(\frac{1}{-x^2+i\epsilon}\right)^{d-1+\gamma_{\mathcal{O}}} = 0 \tag{3.7}$$

[4] In addition, a quartic coupling for the scalar is generated from fermion loops. The quartic coupling also has a non-trivial fixed point. The contributions from the quartic coupling at the fixed point are suppressed by powers of $1/N_c$ and we ignore them for simplicity.

in dimensional regularization. As in the case of free field theory, dimensional regularization automatically discards contributions to the Higgs mass from the cutoff. Of course, we could have also computed this with any other regulator, and we would have determined the Higgs mass counter term to restore scale invariance.

3.3 Higgs mass sensitivity to non-perturbative threshold scales

We now turn to the case of interest: a theory which transitions between two different scaling behaviors at a transition scale M. Since the interacting fixed point for the couplings g and λ of the theory we introduced in the previous section is IR attractive, one could use that theory to construct an example of a model which flows from a free fixed point in the UV to the interacting one in the IR with an associated change in dimension of the operator $\mathcal{O}$. However, we are interested in a theory which is IR free and flows to an interacting UV fixed point because this more similar to what one would expect if the hypercharge $U(1)$ was to merge into a CFT in the UV.

In such a theory, the two-point function (3.6) is of the form

$$\langle 0|T\,\mathcal{O}^\dagger(x)\mathcal{O}(0)|0\rangle = \left(\frac{1}{-x^2}\right)^{d-1} f(-x^2M^2)\ . \tag{3.8}$$

Here, the factor of $(-x^2)^{1-d}$ is determined by dimensional analysis and it coincides with the two-point function in free field theory. The dimensionless function $f(y)$ contains all the information about the interacting dynamics. Since $f(y)$ is defined over all scales it cannot be computed reliably at any fixed order in perturbation theory. At the very least, calculating $f(y)$ requires knowing the solution to the renormalization group equations to determine anomalous dimensions. In a conformal regime, $f(y)$ reproduces the power law corresponding to the anomalous dimension of $\mathcal{O}$. In the transition region between two fixed points, it interpolates between the two power laws appropriate for the fixed points in the

UV and IR[5]

$$f(y) \to \begin{cases} 1 & \text{as} \quad y \to \infty \text{ (IR)}, \\ y^{-\gamma_{\rm UV}} & \text{as} \quad y \to 0 \quad \text{(UV)}. \end{cases} \tag{3.9}$$

For our purposes, the most important feature of the two-point function in (3.8) is that it depends on the transition scale M in a non-trivial way. This M-dependence is what ensures that the $\int d^d x$ integral in (3.8) does not vanish even in dimensional regularization barring fine tuning[6]. This is the main result of this chapter: the Higgs mass does receive quantum corrections proportional to the non-perturbative transition scale M.

To see this more explicitly, we simplify (3.8) by performing a Wick rotation, using the $SO(d)$ symmetry of Euclidean space to do the angular integrals, and changing variables to $y = -x^2 M^2$. Then

$$\begin{aligned} \delta m_h^2 &= -\, i\lambda_t^2 \mu^{4-d} \int d^d x \left(\frac{1}{-x^2}\right)^{d-1} f(-x^2 M^2) \\ &= -\, M^2 \, \frac{\lambda_t^2 \pi^{d/2}}{\Gamma(d/2)} \left(\frac{\mu^2}{M^2}\right)^{2-d/2} \int_0^\infty \frac{dy}{y^{d/2}} \, f(y) \ . \end{aligned} \tag{3.10}$$

We now consider two illustrative examples for $f(y)$ and compute the Higgs mass in each case. We chose our examples based on calculability and their qualitative features. The first example is a crude toy model that is far from realistic, but easy to understand analytically. We assume that the transition between the UV and IR fixed points is abrupt

$$f(y) = \begin{cases} 1 & \text{for} \quad y > 1, \\ y^{-\gamma_{\rm UV}} & \text{for} \quad 1 > y > 0. \end{cases} \tag{3.11}$$

The integral in (3.10) is divergent in the UV (at small y) and requires a regulator. However since the UV behavior of the correlation function is exactly that of a CFT we can use scale invariance of the UV theory to fix the mass counter term to cancel the scale invariance violation from the regulator. A nice way to implement the subtraction by the counter term

[5]Near the free fixed point in the IR the scaling of operators includes logs which we ignore. We will discuss logs near a UV fixed point in the next Section.

[6]An exception arises when the M-dependence is trivial and can be factored out of the integral. Then the integrand does not transition between two different scaling behaviors in the UV and IR, and the corresponding integrals, $\int d^d x (-x^2)^\alpha$, can be set to 0 in dimensional regularization.

is to subtract from (3.10) the corresponding expression in a CFT: $\int dy/y^{d/2}$. This automatically subtracts the correct counter term required by scale invariance of the UV theory in any regularization scheme. Of course, in the special case of dimensional regularization this counter term vanishes so that we simply subtract zero. If after the subtraction we are left with a finite integral then we can evaluate it in four dimensions.

The integral from 0 to 1 is completely removed by the subtraction and the remainder gives

$$\delta m_h^2 = -M^2\pi^2\lambda_t^2 \int_1^\infty \frac{dy}{y^2}\left[1 - \frac{1}{y^{\gamma_{\rm UV}}}\right] = -M^2\pi^2\lambda_t^2 \frac{\gamma_{\rm UV}}{1+\gamma_{\rm UV}}. \tag{3.12}$$

In this case, the main contribution to the Higgs mass can be thought of as coming from the threshold at M (or $y = 1$) where there is an abrupt change of the scaling dimension.

The abrupt transition in our example (3.11) is clearly unphysical and one might think that a smoother and more physical transition would suppress the contributions to the Higgs mass. In fact, we will find the opposite to be true in our next example. We consider the smooth function $f(y)$

$$f(y) = \left(\frac{1}{y^{n\gamma_{\rm UV}} + y^{n\gamma_{\rm IR}}}\right)^{1/n}. \tag{3.13}$$

Assuming that $\gamma_{\rm UV} < \gamma_{\rm IR} \leq 0$, $\gamma_{\rm UV}$ modifies the two-point function at small y, while $\gamma_{\rm IR}$ does so at large y. Meanwhile, the power n controls whether the transition between UV and IR is smooth or abrupt. The larger the n the more abrupt the transition.

Choosing free field theory for the IR, $\gamma_{\rm IR} = 0$, we have

$$\begin{aligned}
\delta m_h^2 &= -M^2\,\frac{\lambda_t^2\pi^{d/2}}{\Gamma(d/2)}\left(\frac{\mu^2}{M^2}\right)^{2-d/2}\int_0^\infty \frac{dy}{y^{d/2}}\left(\frac{1}{1+y^{n\gamma_{\rm UV}}}\right)^{1/n} \\
&\xrightarrow{d=4} -M^2\,\lambda_t^2\pi^2\int_0^\infty \frac{dy}{y^2}\left[\frac{1}{(1+y^{n\gamma_{\rm UV}})^{1/n}} - \frac{1}{y^{\gamma_{\rm UV}}}\right] \\
&= -M^2\,\lambda_t^2\pi^2\,\frac{\Gamma\left(\frac{1}{n}+\frac{1}{n\gamma_{UV}}\right)\Gamma\left(1-\frac{1}{n\gamma_{UV}}\right)}{\Gamma\left(\frac{1}{n}\right)},
\end{aligned} \tag{3.14}$$

where in the second line we first subtracted a quantity which vanishes in dimensional regularization and then set $d = 4$. The subtraction is identical to the contribution to the Higgs mass in a CFT which has identical UV anomalous dimensions to our example theory. It

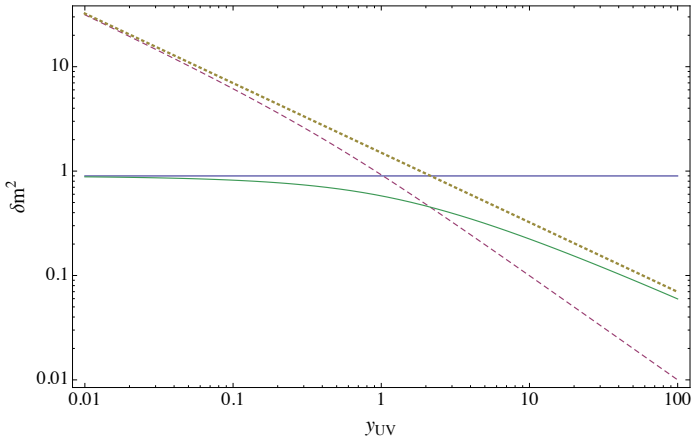

Figure 3.2: Plot of the contributions to the Higgs mass in (3.15) as a function of the UV cutoff $y_{\rm UV}$ on the integral. The blue horizontal line corresponds to the full Higgs mass contribution. The green line which asymptotes to it at small $y_{\rm UV}$ is (3.15) as a function of the short distance cutoff $y_{\rm UV}$. The two lines which grow at small $y_{\rm UV}$ are the original unsubtracted integral (red-dashed) and the subtraction (yellow-dotted), both evaluated with the short distance cutoff. In this example, we chose $n = 4$ for the transition parameter and $\gamma_{\rm UV} = -1/3$ for the UV anomalous dimension.

corresponds to the counter term which is required by scale invariance of the UV theory. The remaining integral is finite for sufficiently large n and $-1 < \gamma_{\rm UV} < 0$.

It is interesting to explore where the main contribution to the Higgs mass comes from. To this end we compute the subtracted integral in (3.15) with a UV cutoff $y_{\rm UV}$. The integral evaluates to a generalized hypergeometric function. We plot it as a function of $y_{\rm UV}$ in Figure 3 for $n = 4$ and $\gamma_{\rm UV} = -1/3$. One sees that the Higgs mass contribution approaches its full value near $y_{\rm UV} = 1$ implying that the bulk of the Higgs mass contribution comes from quantum corrections with energies near the transition scale M. Where exactly the maximum of the contributions comes from depends on the parameters n and $\gamma_{\rm UV}$.

What happens for smaller values of n for which the subtracted integral is not UV finite? For small n the transition between the IR and UV fixed point is relatively slow. As in the top quark loop example in Section 2, conformal invariance is not restored sufficiently rapidly in the UV, and new UV divergences which depend on conformal symmetry breaking arise.

To see these UV divergent contributions explicitly we expand the function $f(y)$ in (3.15) in a series for small y. The leading term is removed by the CFT subtraction. But for small n one or several subleading terms are also UV divergent. These terms give contributions which are proportional to fractional powers of the UV cutoff and of M and are evidence that scale invariance is not restored in the UV. Thus in these examples the Higgs mass suffers from sensitivity to the UV cutoff entangled with the transition scale M.

Can the Higgs mass be suppressed by considering smoother transitions? We have already seen that n needs to be large enough to just obtain a finite contribution. Considering only values of n such that the integral in (3.15) is finite, the magnitude of the Higgs mass contribution increases for smoother transitions (smaller n). This is because smoother transitions increase the width of the transitions region so that contributions from shorter distances can contribute in (3.15).

We close this Section with a comment on the choice of regulator. So far, we have mostly used dimensional regularization and relied on the fact that integrals of power laws, $\int d^dx(-x^2)^\alpha$, can be consistently set to 0 [112]. How would our calculation differ if we used an explicit momentum cutoff Λ?

Considering for example the calculation of the Higgs mass in the smooth transition model we would find

$$\begin{aligned}\delta m_h^2 =& - M^2\lambda_t^2\pi^2 \int_{\frac{M^2}{\Lambda^2}}^\infty \frac{dy}{y^2} f(y) \\ =& - \lambda_t^2\pi^2 \left(\frac{\Lambda^2}{1+\gamma_{UV}} \left(\frac{\Lambda^2}{M^2}\right)^{\gamma_{UV}} + M^2 \frac{\Gamma\left(\frac{1}{n}+\frac{1}{n\gamma_{UV}}\right)\Gamma\left(1-\frac{1}{n\gamma_{UV}}\right)}{\Gamma\left(\frac{1}{n}\right)} + \dots \right),\end{aligned} \tag{3.15}$$

where the dots stand for terms which vanish as we take Λ to infinity. The second term reproduces the dimensional regularization result. The first term arises from the explicit breaking of scale invariance by the cutoff and its apparent M-dependence is a fake which stems from our choice of normalization of the operators $\mathcal{O}$ and H. In our normalization, the operators are normalized to their free (IR) scaling behavior. However, in the UV the operators have anomalous dimensions which modify the divergence to $\Lambda^{2+\gamma_{UV}}$, the explicit power of M in (3.15) arises from the matching of the UV Higgs mass operator to the

IR. Note that the M-dependence of the subleading divergences for small n is different, it corresponds to breaking of scale invariance that persists in the UV.

3.4 Asymptotically free theories

The example theory considered in the previous section has an interacting fixed point in the UV. In the vicinity of an interacting fixed point correlation functions do not exactly obey the power-law scaling in (3.6), but the deviations from such scaling are suppressed by higher powers of x^2. We have already seen that if the approach to the UV fixed point is too slow, i.e. deviations from CFT scaling are not suppressed by sufficient powers of x^2 then the scale invariant UV subtraction is not sufficient to render the Higgs mass finite. In this case the theory requires fine-tuning the UV counter terms to cancel contributions which depend on both the UV and the threshold scale M.

In the case of a free UV fixed point the approach to the free CFT scaling is especially slow. It includes logarithms which break conformal invariance at arbitrarily short distances. We therefore do not have a symmetry which allows canceling the UV contributions to the Higgs mass. As a result it is not possible to disentangle Higgs mass sensitivity to the transition scale M from sensitivity to the cutoff Λ.

To see the problem arise explicitly in a calculation consider again a complex scalar coupled to the "top quark" as in (3.1). For simplicity, assume that "top quark" is massless to avoid the scale invariance breaking from the mass. We assume that the quark has its usual asymptotically free QCD interactions as in the Standard Model, and we are interested in computing the contributions to the Higgs mass from the UV, taking into account the running QCD coupling.

The UV contributions to the matrix element (3.6) can be computed using the operator product expansion. The coefficient of the leading $\mathbf{1}$ operator in $\mathcal{O}^\dagger(x)\mathcal{O}(0)$ gives (see for example Chapter 18.3. in [113])

$$\langle 0|T\,\mathcal{O}^\dagger(x)\mathcal{O}(0)|0\rangle \propto \left(\frac{1}{|x|^2}\right)^3 \left(\log\frac{1}{|x|^2M^2}\right)^{-a/b_0} . \tag{3.16}$$

If we were discussing real QCD, M would be replaced by $\Lambda_{\rm QCD}$, $a = 8$ would be the one-loop anomalous dimension coefficient of $\mathcal{O} = \bar{t}t$, and $b_0 = 7$ for 6 quark flavors. The scale M appears because we have re-summed an infinite class of diagrams to capture the leading x-dependence at small x using the renormalization group.

We now integrate this expression over x, and change variables to $z = 1/x^2$ to obtain

$$\delta m_h^2 \propto \int_{z_{IR}}^{\infty} dz \left(\frac{1}{\log(z/M^2)} \right)^{a/b_0} \quad . \tag{3.17}$$

We also introduced an IR cutoff somewhat above the transition scale M (or $z_{IR} \sim \text{few} \times M^2$) to exclude distance scales from the integration for which the running of the coupling deviates significantly from the one-loop approximation. Assuming that there are no further scales above M one would naively expect this integral to be given by some order one factor times M^2. However, the integral is divergent in the UV and requires regularization.

As discussed earlier, it is not apparent how to do this while keeping the contributions from M and the regulator separate. Evaluating the integral in $d < 2$ dimensions and analytically continuing to $d = 4$ one encounters a multi-valued function with branch cuts in the complex d-plane, which makes the analytic continuation not unique. Subtracting the corresponding integral of the UV CFT ($\int_{z_{IR}}^{\infty} dz\, 1$) to try to restore scale invariance fails because of the inverse logarithm. Evaluating the integral with a momentum cutoff one obtains terms which scale roughly like Λ^2 times inverse powers of $\log(\Lambda^2/M^2)$ in the UV and therefore require M-dependent subtractions to remove the cutoff dependence. In summary, it is not possible to separate cutoff dependence from M dependence because scale invariance is not preserved in the UV. We conclude that theories with coupling constants which approach free fixed points in the UV cannot protect the Higgs mass from fine tuning.

3.5 Conclusions

It has been proposed that if the SM were to merge into a conformal field theory in the UV then the scale invariance of the asymptotic CFT would guarantee the cancelation of UV contributions to the Higgs mass and the Higgs mass could be natural. The proposal

necessarily introduces new UV scales, the scales at which the couplings constants stop running as in the SM model and instead start approaching their UV fixed points. We showed that quantum corrections to the Higgs mass are sensitive to these scales even if there are no massive particles and the scales are of non-perturbative origin.

Therefore, naturalness of electroweak symmetry breaking in the SM requires that any such non-perturbative scales are sufficiently low. In particular, this means that the hypercharge beta function must be modified near the TeV scale and the running of the gravitational coupling must change at or below $\sqrt{M_{\text{weak}} M_{\text{Planck}}}$.

Of course, the beta function of the hypercharge coupling can be computed easily in the Standard Model, and it does not have a UV fixed point. Thus, turning around the coupling at the TeV scale requires new interactions beyond the SM. In principle, gravitational interactions could provide these new contributions to the beta function, however at the TeV scale gravitational interactions are much too weak to be relevant. Hence, new interactions are required near the TeV scale, and it seems that unification of the $U(1)$ into a non-Abelian gauge group is the simplest possibility. Therefore, new weakly-interacting gauge bosons with masses near the TeV scale are expected in theories in which the SM is merged into a CFT in the UV. This is, of course, no different from more conventional approaches to the hierarchy problem in which new particles at the TeV scale are required to fill out multiplets of the symmetry which protects the Higgs mass from quantum corrections.

In addition to the dependence on threshold scales we also showed that anomalous dimensions must approach their UV fixed point values sufficiently rapidly for conformal symmetry of the UV to protect the Higgs mass from divergent contributions from short distances. This rules out even asymptotically free gauge groups as possible ingredients of a UV CFT.

4 Non-Abelian Dark Matter

4.1 Introduction

Dark matter makes up more than 80% of the matter content of our universe [114]. Despite the overwhelming evidence for dark matter (DM), we have only probed it through its gravitational effects which leaves a broad range of possibilities for dark matter models. In particular, there could be a whole dark sector in addition to dark matter consisting of particles which interact only with themselves and with dark matter (see e.g. [115, 116]).

In this work we propose a scenario for the dark sector which leads to very interesting phenomenology and has been overlooked in the dark matter literature. We consider a dark sector with an unbroken non-Abelian dark gauge group and a dark matter which is charged under this group. In addition to this non-Abelian gauge interactions, DM also has non-negligible interactions with the Standard Model, such that the dark sector and the Standard Model were in equilibrium in the early universe. We focus on confinement scales for the dark gauge group that are small compared to the current Cosmic Microwave Background (CMB) temperature. In this scenario the dark gauge bosons (which we will call dark gluons from here on) are a massless degrees of freedom and behave as a non-standard type of dark radiation. It is non-standard since, due to their self-interactions, the dark gluons are described as a perfect fluid instead of a free-streaming fluid, which leads to distinct imprints in the CMB [117].

We also explore the effects of the interactions between dark radiation and dark matter in the matter power spectrum. The interaction rate between non-Abelian dark radiation and DM has interesting scaling with the temperature, which has not been studied in the past and leads to new effects in the power spectrum. This is because instead of leading to the usual cutoff in the power spectrum at the scale in which DM and DR decouple [118], this interaction leads to a smooth reduction of the power spectrum at small scales in a regime in which DM and DR are only partially coupled. This is an interesting new behavior and

could resolve the tension between Planck data and measurements of Power Spectrum at small scales (see e.g. [114, 119, 120]).

Most of the features associated with non-Abelian dark matter are generic, but in order to make such effects concrete we will study a specific example in this chapter. We will focus on a WIMP dark matter charged under a hidden $SU(N)$ gauge group. We will briefly discuss the implications of this non-Abelian nature of DM to the standard WIMP searches. Then we will investigate the effects of the dark radiation in the CMB and also of the interactions between DM and DR to the matter power spectrum. We will show that the effects on the CMB restrict N to be smaller or equal to 3 and also limit the dark sector coupling constant α_d to be smaller than $\sim 10^{-7}$.

4.2 The Model

For concreteness we will focus on a specific realization of a non-Abelian dark matter model. We take the dark matter particle to be a vector-like fermion in the $(1,3)_0$ representation of the Standard Model gauge group and in the fundamental representation of the dark $SU(N)$. It has an $SU(2)_W$ preserving Dirac mass M_χ and no additional interactions with the Standard Model besides gauge interactions. Due to Electroweak symmetry breaking there is a mass splitting between the neutral and charged components of the $SU(2)$ triplet with the neutral component being lighter. In the limit $M_\chi \gg M_W$ the splitting is independent of M_χ and given by [121]

$$\delta M_\chi = M_{\chi^\pm} - M_{\chi^0} \approx 0.16\,\mathrm{GeV}\,. \tag{4.1}$$

The neutral component χ^0 is dark matter and it is automatically stable because of its $SU(N)$ charge. At the time of DM chemical freeze-out, $T \gg \delta M_\chi$, and thus we can ignore the splitting between the different components of χ^a when calculating the relic abundance. Once the temperature drops below δM_χ, all the charged components of χ decay to χ^0 and hence $n_{\chi^a} \to n_{\chi^0}$. This explains why we can use the abundance calculation for the whole triple χ^a in order to find the dark matter relic abundance.

The dark gauge coupling is much smaller than the SM gauge couplings and therefore the relevant interactions for the thermal relic calculations are of the form $\chi\chi \to$ SM SM and to leading order independent of the dark gauge coupling. Figure 4.1 shows some of the relevant diagrams for DM annihilating to SM particles. If the DM mass is much larger than M_W, the thermally averaged effective annihilation cross-section is given by

$$\langle \sigma v \rangle = \frac{1}{2N} \frac{37 g_2^4}{192 \pi M_\chi^2} \,, \tag{4.2}$$

where g_2 is the $SU(2)_W$ gauge coupling. This cross-section differs from the standard $SU(2)$ triplet fermion DM [122] by the extra $1/2N$ factor, which comes from the multiplicity associated with the $SU(N)$ representation and the fact that χ is a Dirac instead of a Majorana fermion. This factor can be easily understood from the fact that a given DM particle now carries an extra dark color charge and can only annihilate if it finds an anti-particle with the right anti-dark color, thus reducing the color averaged annihilation cross-section.

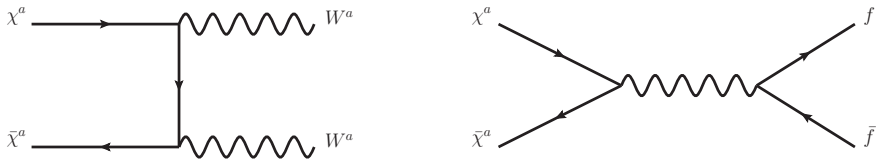

Figure 4.1: Annihilation of dark matter to $SU(2)_W$ gauge bosons and to SM fermions.

It is well known that if DM gets its abundance from a thermal freeze-out process, its abundance today depends, to a good approximation, only on its annihilation cross-section [18]. Therefore, from Eq. 4.2 we see that the mass required to get the correct relic abundance decreases as the square root of N. In Table 4.1 we show the mass of DM for different values of N using the tree level annihilation cross-section. Those masses are significantly lower than the usual non-$SU(N)$ case, which at tree level is 2.4 TeV (and about 3 TeV if one includes Sommerfeld enhancement [123]).

$N = 2$	$N = 3$	$N = 4$	$N = 5$	Generic N
1.2 TeV	1.0 TeV	0.9 TeV	0.8 TeV	$\sim \frac{2.4}{\sqrt{2\,N}}$ TeV

Table 4.1: Dark Matter masses required to get the correct thermal abundance as a function of N ignoring Sommerfeld enhancement.

4.2.1 Dark Matter multiplicity and experimental searches

Because we are working in the limit of very small dark gauge couplings the only relevant effect of the dark $SU(N)$ to DM searches comes from the fact that dark matter comes in dark color multiplets, i.e. there is a multiplicity associated with DM. The leading effect of this multiplicity is to reduce the DM mass, which can lead to large changes in sensitivity from different experiments. In addition, we have already seen in the thermal abundance calculation that this leads to trivial multiplicity/color factors in cross-sections associated with DM interacting SM processes. Figure 4.2 shows the color factors associated to the different kinds of DM searches. In what follows we briefly describe the effects of $SU(N)$ multiplicity for Direct and Indirect Detection and also for Collider Searches for DM:

Direct detection: For direct detection there is no color factor associated with the multiplicity, thus the only change comes from dark matter being lighter. The spin-independent cross-section for dark matter scattering of the nucleus is approximately $10^{-47}\,\mathrm{cm}^2$, and independent of the DM mass as long as $M_\chi \gg M_W$ [124]. This cross-section is an order of magnitude smaller than the projected sensitivity of the next generation direct detection experiments. However, in the mass range of interest (around 1 TeV) it is above the neutrino background and potentially within reach of future experiments [125].

Collider searches: The multiplicity factor enhances sensitivity for collider searches in two ways. It decreases the DM mass, and thus a lower center of mass energy is required to pair produce DM. This is a big enhancement since the effective luminosity changes vary rapidly with the center of mass energy. It also increases the cross-section for pair

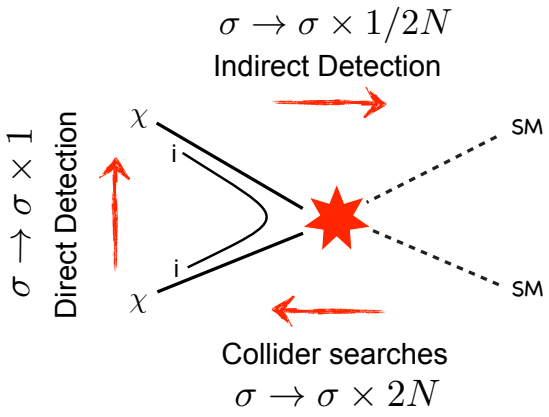

Figure 4.2: Color factors for the different types of DM search experiments. The different multiplicity factors can be easily understood from the color flow in the figure. For direct detection the color of the incoming dark matter is the same as of the outgoing and so there is no multiplicity factor. For indirect detection it is an annihilation diagram, so just as for the thermal relic calculation there is a $1/2N$ suppression because a DM particle can only annihilate if it finds the anti-particle with the right anti-dark color. For colliders there is an $2N$ enhancement because any of the different N colors can be created and an extra 2 from Dirac vs Majorana.

producing dark matter by a factor of $2N$. Despite this gain in sensitivity the mass range of interest is still out of reach of the LHC, but should be within easy reach of the proposed 100 TeV collider (see e.g. [126, 127]). Another potentially interesting signature of this model is to look for modifications to the running of the EW gauge coupling [128]. The multiplicity of DM leads to an $2N$ enhancement factor in the DM contribution to the α_2 running at one loop, which would lead to significant effects in the proposed 100 TeV collider.

Indirect Detection: The annihilation cross-section relevant for indirect detection gets suppressed by a $1/2N$ factor. If one includes Sommerfeld enhancement then the cross-section is further reduced when compared to the non-$SU(N)$ model. This is because there is a large Sommerfeld enhancement when the dark matter mass is in

the $2-3$ TeV range, and the effect is much smaller for masses around 1 TeV. The non–$SU(N)$ case has been widely investigated recently [129–132], and is strongly disfavored by H.E.S.S data. The non-Abelian case is not constrained by either H.E.S.S or Fermi data for the values of N under consideration, but the annihilation cross-section is close to H.E.S.S sensitivity and should be within reach of CTA [131, 133].

4.3 Dark gluons as Dark Radiation

In this section we turn our attention to the evolution of the dark gluons and its effects on the CMB. In order to study the effects of the dark gluons on the CMB we first need to know its temperature compared to the photon plasma.

The dark gluons interact with the dark matter which is in equilibrium with the SM in the early universe. If the dark coupling constant α_d is sufficiently large, the dark gluons will have the same temperature as the SM plasma at early times and thus T_d will not a free parameter. Because we are interested in the limit $\alpha_d \ll \alpha_s$, the most efficient diagram for keeping the dark gluons in chemical and kinetic equilibrium with the SM is the one shown in Figure 4.3. At temperatures much higher than M_χ, the thermally averaged cross-section for this process times the DM number density is given by

$$n_\chi \langle \sigma v \rangle = \lambda \, T^3 \frac{\pi \alpha_W \alpha_d}{N T^2}, \tag{4.3}$$

where λ is an order 1 number. Comparing this to H, we find that the dark gluons will be in equilibrium with the SM at $T \sim M_\chi$ as long as

$$\alpha_d \gtrsim \frac{1}{\alpha_W} \frac{M_\chi}{M_{\rm Planck}}.$$

We see from the equation above that even for α_d as small as 10^{-13} the dark gluons will be in chemical and thermal equilibrium with the Standard Model down to temperatures of about 1 TeV. Once the dark matter becomes non-relativistic its number density drops exponentially and the rate for the process in Figure 4.3 becomes

$$n_\chi \langle \sigma v \rangle = \lambda' (M_\chi T)^{3/2} \, e^{-M_\chi / T} \left(\frac{\pi \alpha_W \alpha_d}{M_\chi^2} \right). \tag{4.4}$$

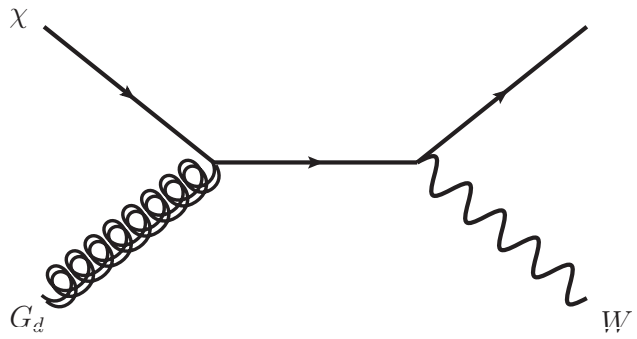

Figure 4.3: Most effective process in keeping dark gluons in equilibrium with dark matter and SM plasma.

The dark gluons decouple at temperatures of about M_χ for $\alpha_d \sim 10^{-13}$ to about $M_\chi/20$ for $\alpha_d \sim 10^{-5}$. Below the decoupling temperature the dark gluon fluid evolves independently with a temperature T_d which redshifts as $1/a$.

The temperature of the photon fluid also redshifts as $1/a$ for most of the universe's evolution. However, because it is coupled to particles that become non-relativistic and start annihilating into lighter particles also coupled to the photon plasma, this effectively heats up the photons compared to the dark gluons (similarly to what happens to photons and neutrinos after neutrino decoupling [18]). The ratio between the photons and dark gluons temperatures can be easily calculated in the instantaneous decoupling approximation by requiring that the entropy per comoving volume is conserved independently in each fluid,

$$\frac{T_d}{T_\gamma} = \left(\frac{g_*^f}{g_*^i}\right)^{1/3}, \tag{4.5}$$

where g_*^i is the number of effective degrees of freedom in the SM plasma at the time of dark gluon decoupling and g_*^f the number of effective degrees of freedom at the time of interest.

The CMB places strong constraints on the number of relativistic degrees of freedom at the time of recombination. This constraint is usually presented as a constraint in the number of effective neutrino species, N_{eff}. The contribution of the dark gluons to N_{eff} is given by

$$\Delta N_{eff} = \frac{8}{7}\left(N^2 - 1\right)\left(T_d/T_\nu\right)^4, \tag{4.6}$$

where the N^2-1 is the number of generators of $SU(N)$ and T_ν is the neutrino temperature. The ratio can be calculated using Eq. 4.5 right before neutrino decoupling when neutrino and photon temperatures are still the same. Assuming the decoupling between dark gluons and the SM happens at temperatures around 50 GeV one finds

$$\Delta N_{eff} = 0.07\,(N^2 - 1).$$

The strongest constrain on N_{eff} comes from the 2015 Planck data [114], which found $N_{eff} = 3.15 \pm 0.46$ with 95% confidence level. We see that this rules out $N \geq 4$ and that the case $N = 3$ is just within the 2σ allowed range. It is worth noting that this measurement assumes the ΛCDM model with a variable N_{eff}, and thus could be potentially relaxed in a modified scenario as the one considered in this chapter.

The effects of dark radiation can be divided as background effects and perturbation effects. The background effects are solely due to a change in the average energy density of relativistic degrees of freedom and are not sensitive to specific properties of the dark radiation fluid. The largest impact of extra relativistic degrees of freedom is changing the redshift of matter radiation equality z_{eq}, and can be canceled by a simultaneous change in the matter density (see e.g. [134–136]). This change in the matter density can be achieved by a change in the Hubble parameter today H_0, while holding Ω_m fixed (the ratio between the matter density and the critical density), which leads to a degeneracy in the CMB data between N_{eff} and H_0.

The perturbation effects are due to perturbations in the dark radiation fluid and thus sensitive to properties of dark radiation. In particular there are two parameters one can use to describe different types of dark radiation, see e.g. [117], the effective sound speed c^2_{eff} and the viscosity speed c^2_{vis}. The dark gluons are a relativistic fluid and have $c^2_{\text{eff}} = 1/3$, which is the same as neutrinos. But because the dark gluons are non-Abelian gauge bosons they interact with one another. If the rate for this interaction is large compared to Hubble the dark gluons can be described as an ideal fluid instead of a free-streaming fluid as neutrinos. This leads to $c^2_{\text{vis}} = 0$ instead of $1/3$ as for neutrinos. The interaction rate between dark

gluons is approximately given by

$$\tau^{-1} \sim \alpha_d^2 T_d, \tag{4.7}$$

and one can see that as long as $\alpha_d \gtrsim 10^{-13}$ this rate is larger than H during recombination. This shows that in the time scale set by Hubble, the dark gluons behave as a perfect fluid. This in turn leads to less damping in overdensities due to relativistic particles streaming out of gravitational potential wells, leading to higher CMB peaks compared to the case of free-streaming dark radiation.

The Planck collaboration has studied the effect of varying c^2_{eff} and c^2_{vis} with N_{eff} fixed to the SM value 3.04, i.e. no dark radiation, and found that it is in perfect agreement with the expected value for neutrinos, $c^2_{\text{eff}} = c^2_{\text{vis}} = 1/3$. If future experiments find a non-zero contribution to dark radiation from the CMB one can use measurements of c^2_{vis} of this extra component to distinguish between dark gluons vs free-streaming dark radiation, like dark photons or sterile neutrinos [117, 137].

4.4 Dark matter-dark gluon interactions and Large Scale Structure

In this section we will study the effects of the interaction between dark gluons and dark matter on the evolution of dark matter overdensities. Because of the dark gluon t-channel exchange shown in Figure 4.4, the interaction rate for DM-DR scattering has a very different scaling dependence on the temperature from what has been explored in the literature (see e.g. [117, 138]), and leads to larger effects at low temperatures.

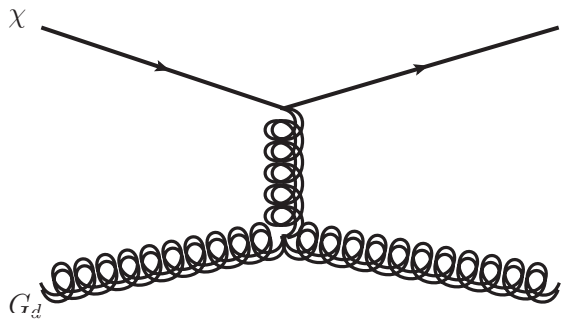

Figure 4.4: t-channel diagram interaction between dark matter and dark gluons.

One measurement of the strength of this interaction is given by the momentum exchange rate [139]. At sufficiently low temperatures this rate is dominated by the t-channel diagram of Figure 4.4 and given by

$$\begin{aligned}\frac{\langle dp_\chi^2/dt\rangle}{\langle p_\chi^2\rangle} =& \frac{1}{3n_\chi M_\chi T_\chi}\int \frac{d^3p_\chi d^3k_d}{(2\pi)^6 2E_p 2E_k} f_\chi(p_\chi) f_d(k_d) \times \\ & \int \frac{d^3p'_\chi d^3k'_d}{(2\pi)^6 2E_{p'} 2E_{k'}} (2\pi)^4\delta^4(p+k-p'-k')(\vec{p}-\vec{p}')^2\,|\mathcal{M}|^2 \\ \approx& \frac{2\pi n_\gamma\,\alpha_d^2 \log 1/\alpha_d}{3M_\chi T_\chi} \\ \approx& \frac{4\zeta(3)}{3\pi}\,\frac{\alpha_d^2 \log \alpha_d^{-1} T_d^3}{M_\chi T_\chi}\,,\end{aligned} \tag{4.8}$$

where f_χ and f_d are the equilibrium distribution functions for the dark matter and dark gluons and n_χ and n_γ are the number densities of the dark matter and dark gluons. The $\log\alpha$ appears because we used the Debye mass $m_d = gT$ of the dark gluons to regulate the t-channel divergence of the diagram in Figure 4.4. In the expression above we kept only the log enhanced terms and also neglected sub-leading terms in T_d/M_χ and T_χ/M_χ.

If for $T_\chi = T_d$ this rate is larger than Hubble, the interaction keeps the dark matter in kinetic equilibrium with the dark gluons. Note that if one sets $T_\chi = T_d$, the momentum exchange rate is proportional to $T_d^2 \propto a^{-2}$, i.e. it has the same scaling as the Hubble expansion rate during radiation domination. This implies that if the momentum exchange rate is large enough to keep DM in equilibrium with DR at early times then DM will stay in equilibrium with DR until at least matter radiation equality. In this case, the pressure from the dark gluons prevents dark matter overdensities from growing which leads to a sharp decrease in the DM power spectrum as can be seen in Figure 4.5. Such a large modification to the power spectrum is in strong disagreement with LSS data and therefore rules out $\alpha_d >\sim 10^{-7}$.

The effects of this interaction are more subtle in the other limit $\alpha <\sim 10^{-7}$. In this case the momentum exchange between the two fluids is not large enough to bring DM to equilibrium with the dark gluon bath. In this case the DM temperature redshifts as a^{-2}, while $T_d \propto a^{-1}$. From Eq. 4.8 one sees that this leads to a momentum exchange rate that

scales as $T_\gamma \sim 1/a$, while the Hubble rate during radiation domination scales as T_γ^2. Because the Hubble rate decreases faster with lowering the temperature, the momentum exchange rate can become larger than Hubble at low temperatures even for $\alpha <\sim 10^{-7}$. Once this happens the interactions with the dark gluons become important and the DM temperature scaling changes from a^{-2} to a^{-1}, keeping the ratio T_d/T_χ fixed.

In order to determine the effect of the interactions to the DM overdensities in this regime we need to write down the linearized evolution equations for the overdensities including the interactions between the DM and DR fluids. In what follows we follow [140] and work in Conformal Newtonian gauge. We study a simplified scenario in which all the SM radiation is made up by photons and all matter is made of dark matter. We treat the photons as a perfect fluid (zero viscosity), since this is a good approximation before recombination, and since after recombination photons contribute a negligible amount to the energy density and thus to the evolution of DM overdensities. In Fourier space the equations for the DM and DR overdensities are

$$\begin{aligned}
\dot{\delta}_{DM} &= -\theta_{DM} + 3\dot{\psi} \\
\dot{\theta}_{DM} &= -\frac{\dot{a}}{a}\theta_{DM} + a\tau_c^{-1}(\theta_{DR} - \theta_{DM}) + k^2\Psi \\
\dot{\delta}_{DR} &= -\frac{4}{3}\theta_{DR} + 4\dot{\psi} \\
\dot{\theta}_{DR} &= k^2\frac{\delta_{DR}}{4} + k^2\psi + \frac{3}{4}\frac{\rho_{DM}}{\rho_{DR}}a\tau_c^{-1}(\theta_{DM} - \theta_{DR})\,,
\end{aligned} \tag{4.9}$$

where the dot represent derivative with respect to conformal time, ρ_{DM} and ρ_{DR} are the average energy densities of DM and DR respectively and δ_X and θ_X are related to the overdensity and velocity divergency in fluid X. We have also set the two metric perturbations equal because we are treating the photons and dark radiation as ideal fluids (no anisotropic stress) and did not include neutrinos which have sizable anisotropic stresses. The interaction between dark matter and dark radiation is encoded in the coefficient τ_c^{-1} [141], which under the same approximations used in Eq. 4.8 is given by

$$\tau_c^{-1} = \frac{\alpha_d^2 \log 1/\alpha_d}{36\pi}\,\frac{T_d^2}{M_\chi} \tag{4.10}$$

The effect of the interactions for different values of α_d can be seen in Figure 4.5, where we

fixed the $M_\chi = 1\,\mathrm{TeV}$ and $N = 2$. One sees that for $\alpha_d = 10^{-7}$ there is a large suppression in the power spectrum for modes with $k > 10^{-2}\,\mathrm{Mpc}^{-1}$ as expected since in this case DM is in equilibrium with the dark radiation bath. We see that there is a smaller suppression of the power spectrum for $\alpha_d < 10^{-7.5}$, also for modes with $k > 10^{-2}\,\mathrm{Mpc}^{-1}$.

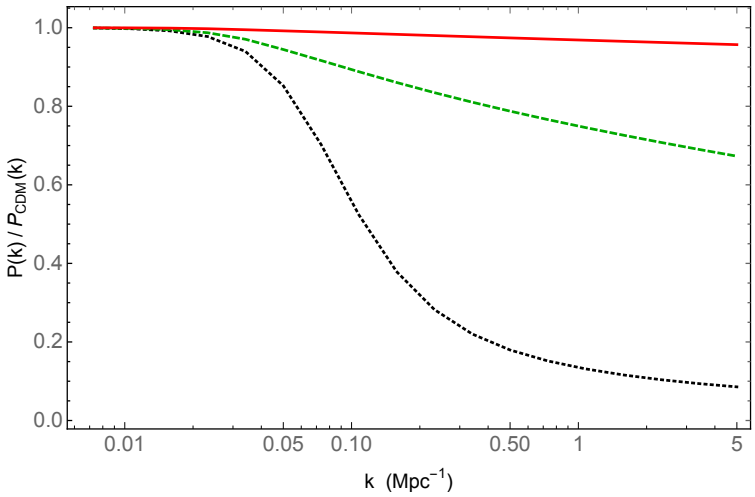

Figure 4.5: Power spectrum including the DM-DR interactions normalized by the CDM power spectrum. The black dotted curve corresponds to $\alpha_d = 10^{-7}$, the green dashed curve corresponds to $\alpha_d = 10^{-7.5}$ and the red line corresponds to $\alpha_d = 10^{-8}$. The power spectrum was defined as proportional to δ^2_{DM} at $a = 10^{-3}$.

Currently there is tension between Planck data and Small Scale Structure data [114, 119, 120]. One measure of the power spectrum for small scales is σ_8, which is a measurement of the matter fluctuations in spheres of radius of $8h^{-1}\,\mathrm{Mpc}$. This tension helps drive Plancks fit for N_{eff} and H_0 to lower values, since larger values of those parameters leads to an increase in Plancks prediction for σ_8 (due to an increase in the total matter density). Therefore a reduction of the power spectrum at small scales due to DM-DR interactions can alleviate tension between Planck and LSS data and also potentially allow larger values of N_{eff}, as is required to account for the dark gluons. An increase in N_{eff} requires increasing H_0 in order to keep the position of the acoustic peaks fixed [114, 134–136]. Increasing Plancks fit for H_0 also lead to better agreement between Planck and Super Nova data [114]. A more quantitative statement about this issue requires a including non-Abelian dark radiation to

a full Boltzmann code and is left to future work.

4.5 Conclusions

In this work we have studied a new type of dark sector, consisting of a $SU(2)_W$ triplet dark matter charged under an unbroken dark $SU(N)_d$ gauge theory. We focused on the scenario in which the confinement scale of the $SU(N)_d$ is much smaller then the current CMB temperature.

We studied the changes in the usual WIMP searches (direct and indirect detection and collider searches) that are related to the fact that dark matter comes in dark color multiplets. This multiplicity leads to color factors that enhance pair production and decrease pair annihilation. The main effect of this is that the DM mass required in order to get the right abundance decreases by $\sqrt{2\,N}$. It also increases the collider cross-section, making this type of dark matter within easy reach of the proposed 100 TeV collider. The decrease in mass and in annihilation cross-section also removes the current tension between thermally produced $SU(2)_W$ triplet dark matter and H.E.S.S data.

We studied the dark gluons contribution to the N_{eff} measured by Planck. This constrained N to be at most 3. We also argued that because of its self interactions the dark gluons leave an imprint in the CMB distinct from that of free-streaming fluids like neutrinos or dark photons. This can be used to distinguish between the two types of radiation if future experiments measure a non-zero contribution to N_{eff}.

We also studied the effects of the interactions between dark matter and dark radiation in the power spectrum. We found that for $\alpha_d \gtrsim 10^{-7}$ this interactions lead to a large suppression of the power spectrum of modes entering the horizon before matter radiation equality and thus such couplings are ruled out. On the other hand, for $\alpha < 10^{-7}$ the interactions lead to a smooth decrease in the power spectrum of small scale modes, which can potentially solve the discrepancy between Planck and small scale structure data and the discrepancy between Planck's and Supernova measurements of H_0. Further investigation of this is left to future work.

Appendices

A Ultraviolet Complete Axigluon Models

In this Appendix we present two complete models for the axigluon and discuss their connection to the simplified models described in section 2.4. In both models the axigluon arises from the breaking of a larger gauge group $SU(3) \times SU(3)$ to the diagonal $SU(3)$, which corresponds to the QCD gauge group. The first model has a parity symmetry built in under which the axigluon is odd. Parity ensures that the light quarks have axial couplings to the axigluon. In this model all particles couple to the axigluon with couplings that are bounded by g_s. In the second model there is no parity symmetry and getting axial couplings to the axigluon requires fine tuning. On the other hand it is easy to introduce particles with large couplings to the axigluon. This is desirable because if these particles are light then the axigluon can have a large partial width to decay to them as required in models A and B in Section 2.4.

A.1 Parity symmetric two site model

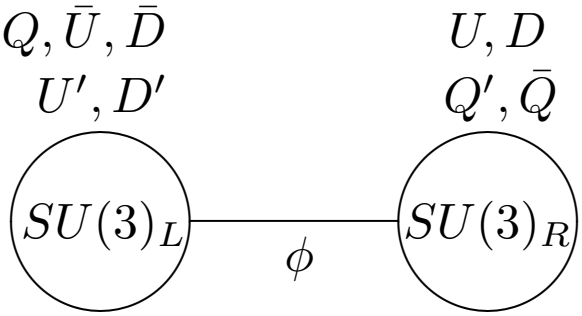

Figure A.1: Moose diagram for the parity symmetric two site model.

This model can be described by the diagram in Figure A.1. There are two $SU(3)$ groups with equal gauge couplings. There is a scalar field ϕ which is a fundamental under $SU(3)_L$ and an anti-fundamental of $SU(3)_R$. The Q is a left-handed Weyl fermion transforming as a fundamental of $SU(3)_L$, and it has the same electroweak quantum numbers as the SM quark

doublets. The fields U and D are right-handed Weyl fermions, transform as fundamentals of $SU(3)_R$ and have the electroweak quantum numbers of the up-type and down-type SM quark singlets. In addition, there are vector-like partners for each of these fields, e.g. (U', $\overline{U}$) are the partners of U. The primed fields are fundamentals under the opposite $SU(3)$ and have the same chirality and electroweak quantum numbers as their unprimed partners. The barred fields have the same chirality and the opposite gauge quantum numbers as the primed fields so that, for example, U' and $\overline{U}$ can have a mass term $M\overline{U}U'$.

This model has a parity symmetry which corresponds to flipping the diagram in Figure A.1, e.g., $Q \leftrightarrow (U, D)$ and $A_L \leftrightarrow A_R$. Clearly this cannot be an exact symmetry because Q and (U, D) have different electroweak quantum numbers (the same reason why parity is not a good symmetry of the SM). Nonetheless, we assume that it is a symmetry of the extended strong interactions and corrections due to the weak interactions are small (suppressed by a loop factor).

The gauge groups are broken to the diagonal by the VEV of the scalar, $\langle\phi\rangle = f\, I_{3\times3}$. This gives a mass $m_A = \sqrt{2}gf$ to the anti-symmetric combination $A^\mu = \frac{1}{\sqrt{2}}(A_L^\mu - A_R^\mu)$ and leaves the symmetric combination massless. The massive vector A_μ is the axigluon and the massless one the gluon G_μ. Fields charged under $SU(3)_{L/R}$ couple to the axigluon with couplings $\pm g_s = \pm g/\sqrt{2}$.

In order to get suppressed couplings of the SM quarks to axigluons we now introduce mixing between the fermions. Since the fermions and their partners have opposite sign couplings to the axigluon any linear combination of the two will have a reduced coupling. The mixing is obtained by adding a Yukawa coupling involving the link field ϕ in addition to the Dirac mass of U' with $\overline{U}$, e.g.

$$\mathcal{L} = \overline{U}\left(MU' + \lambda\phi U\right) + h.c.. \tag{A.1}$$

After plugging in the VEV for ϕ one sees that the combination $U_H = \cos\alpha U' + \sin\alpha U$ gets a mass $M_{HQ} = \sqrt{M^2 + \lambda^2 f^2}$ with $\overline{U}$, where $\tan\alpha = \lambda f/M$. The orthogonal combination $U_{SM} = \cos\alpha U - \sin\alpha U'$ remains massless and corresponds to the SM quark; it eventually

gets a mass from the SM Higgs VEV via Yukawa couplings which we have not explicitly displayed here.

The couplings of the mass eigenstates to the axigluon are given by

$$\mathcal{L} = g_s A^a_\mu \left[\cos(2\alpha) U^\dagger_H \sigma^\mu T^a U_H - \cos(2\alpha) U^\dagger_{SM} T^a U_{SM} - \sin(2\alpha)(U^\dagger_H \sigma^\mu U_{SM} + h.c.)\right]. \quad \text{(A.2)}$$

We see that the axigluon coupling to SM quarks is $g_A = g_s \cos 2\alpha$. By choosing appropriate values for α we can obtain $g_A \simeq 0.3 - 0.5$ as required to explain the $t\bar{t}$ asymmetry. The couplings of the axigluon to SM quarks are automatically axial as long as the mass and Yukawa terms A.1 for the left-handed, Q and right-handed fermions (U, D) and their respective partners respect the parity symmetry. The axigluon also has mixed coupling allowing transition between a SM quark and its heavy quark partner with $g_{mix} = -\sin(2\,\alpha) g_s$, the couplings satisfy the relation $g_s^2 = g_A^2 + g_{mix}^2$.

To summarize, this extension of the SM contains an axigluon with mass $2g_s f$. The SM quarks get their masses from the Higgs VEV as usual and couple axially to the axigluon with coupling $g_A = g_s \cos(2\alpha)$. The model contains heavy partner quarks[1] with masses $M_{HQ} = \sqrt{M^2 + \lambda^2 f^2}$. The axigluon has mixed couplings to SM quarks and their heavy partners with $g_{mix} = -g_s \sin(2\alpha)$. It also couples to two heavy quarks with couplings $-g_A$ (to U_H) and g_s (to $\overline{U}$).

A.1.1 Connection with the simplified models of Section 2.4

The model discussed in this section provides a good skeleton for building complete versions of the simplified models C and D presented in Section 2.4. The coupling λ_m between the axigluon, a quark and its heavy partner is fixed to be $g_{mix} = -g_s \sin(2\alpha)$. Because this coupling is bounded by g_s one needs multiple flavors of heavy quarks being lighter than the axigluon in order to generate a large enough partial decay width of axigluons to quarks and their heavy partners.

[1] As it stands this model has gauge anomalies. The anomalies can easily be cancelled with additional chiral fermions which are vector-like under the SM gauge group. Their mass must be proportional to the ϕ VEV and is bounded by $4\pi f$. Therefore these fermions can be pair-produced at the LHC. For simplicity, we assumed that they are too heavy to play a role in axigluon phenomenology.

As discussed in the Lagrangian description of scenario C we choose all partners of the 1st and 2nd generation right-handed quarks to be degenerate and light, this corresponds to 4 heavy quarks lighter than the axigluon. Notice that this explicitly breaks the parity symmetry in the axigluon sector, since we are treating the partners of U's and D's differently than the partners of Q's. This leads to some fine-tuning in order to preserve the purely axial couplings of the axigluon to SM quarks. Models with more sophisticated flavor structure than the one presented here might allow one to preserve the parity symmetry. We did not pursue this issue further in this thesis.

If the "axion", η, which is a component of the link field ϕ, is given a mass larger than that of the lightest heavy quark than one has an implementation of model C. If the axion is lighter than the heavy quark one has an implementation of model D, with the couplings of η to SM quarks induced by the Yukawa interaction in Eq. A.1.

A.2 Asymmetric two site model

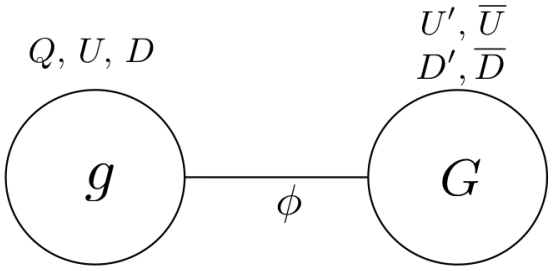

Figure A.2: Moose diagram for the asymmetric two site model.

This model can be described by the diagram in Figure A.2. The axigluon also arises from the breaking $SU(3)_1 \times SU(3)_2 \to SU(3)_{\text{Color}}$. However in this case the gauge couplings are not equal and thus the linear combinations corresponding to the gluon and the axigluon are no longer symmetric and anti-symmetric in A_1 and A_2. Defining $\tan\beta = g/G$ we have

$$G^\mu = \cos\beta A_1^\mu + \sin\beta A_2^\mu \,, \qquad A^\mu = \sin\beta A_1^\mu - \cos\beta A_2^\mu \,. \tag{A.3}$$

The axigluon mass is $m_A = \sqrt{g^2+G^2}f$, and the strong coupling is given by $g_s = \frac{gG}{\sqrt{g^2+G^2}}$.

In this model there are left-handed fermions Q and right-handed fermions U, D all charged under $SU(3)_1$. They end up with couplings to the axigluon given by $\frac{g}{G}g_s$ which can be made smaller than g_s simply by taking $g < G$. This is nice because small axigluon couplings are needed to explain the $t\bar{t}$ asymmetry. The problem is that the couplings are purely vectorial. This can be fixed by introducing fermion mixing. For definiteness we choose to only mix the right-handed fermions U, D with right-handed heavy fermions U', D' charged under $SU(3)_2$. The massless combinations which are identified with the SM fields are $U_{SM} = \cos\alpha U - \sin\alpha U'$ and $D_{SM} = \cos\alpha D - \sin\alpha D'$. Their couplings to the axigluon are given by

$$g_A^R = g_s\left(\frac{g}{G}\cos^2\alpha - \frac{G}{g}\sin^2\alpha\right), \tag{A.4}$$

where α is the mixing angle between unprimed and primed fields. We see that by fine-tuning the mixing angle so that $\sin\alpha = \sqrt{2}g/\sqrt{g^2+G^2} = \sqrt{2}g_s/G$ one can obtain axial couplings between the axigluon and the SM quarks.

Notice that any particle which is charged only under $SU(3)_2$ couples to the axigluon with coupling $-g_s\,G/g$. Therefore one can easily introduce particles that couple strongly to the axigluon by making them charged under $SU(3)_2$. This allows for a large decay width of the axigluon to such particles if they are lighter than the axigluon.

The Lagrangian describing the couplings of the axigluon to the gluon is then

$$\begin{aligned}\mathcal{L} = &-\frac{1}{2}\mathrm{tr}(F^{\mu\nu}F_{\mu\nu}) + m_A^2\mathrm{tr}(A^\mu A_\mu) + ig_s\mathrm{tr}\left(G_{\mu\nu}[A^\mu,\,A^\nu]\right)\\ &+ ig_s\left(\frac{g}{G}-\frac{G}{g}\right)\mathrm{tr}\left(F_{\mu\nu}[A^\mu,\,A^\nu]\right) + \frac{g_s^2}{2}\left(1+\frac{(G^2-g^2)^2}{G^2g^2}\right)\mathrm{tr}\left([A_\mu,\,A_\nu]^2\right),\end{aligned} \tag{A.5}$$

where $G_{\mu\nu}$ is the gluon field strength and $F_{\mu\nu} = D_\mu A_\nu - D_\nu A_\mu$ is the axigluon field strength. The third term in the equation above is the χ-term of Eq. 2.2 with $\chi = 1$ as required by unitarity. The fourth term contains a triple axigluon vertex and is absent in the parity symmetric limit when $g = G$.

This model is another example of a UV completion for the axigluon model. The mass of the axigluon is given by $m_A = \sqrt{g^2+G^2}\,f$. In addition to the SM quarks there are heavy

vector-like partners for all right-handed SM quarks (note that this was an arbitrary choice, there could instead be partners for the left-handed quarks or for both). The couplings of SM quarks to the axigluon are naturally suppressed, but in order to obtain axial couplings one needs to fine tune the quark mixing angle α. Despite this ugly fine tuning this model has a few advantages over the previous one: it requires a smaller number of extra particles, one can easily introduce decay channels with large partial widths for the axigluon, and the fermion assignments are automatically anomaly free.

A.2.1 Connection with the simplified models of Section 2.4

Using the construction described in this section one can easily implement a complete version of models A and B of Section 2.4, which require large couplings of new intermediate resonances to the axigluon. To implement Model B we take the mass of the heavy partner of the bottom quark to be smaller than half the axigluon mass and all other heavy quarks heavier than the axigluon. We also choose $\sin\alpha = \sqrt{2}g_s/G$. The couplings of the axigluon to the heavy quarks defined in Eq. 2.4 are then

$$\lambda_H = g_s \frac{G}{g}\left(2\frac{g^2}{G^2} - 1\right), \quad \overline{\lambda}_H = g_s\frac{G}{g}, \quad \lambda_{mix} = g_s\sqrt{2 - \frac{2g^2}{G^2}}\,. \tag{A.6}$$

We see that one automatically has a large coupling (since we are taking $G > g$) of the axigluon to two heavy quarks as required in model B.

In order to implement model A one assumes that all heavy quarks are heavier than the axigluon, so that it cannot decay to heavy quarks. Then one includes an additional scalar π which is an adjoint of $SU(3)_2$ and not charged under $SU(3)_1$. After the breaking $SU(3)_1 \times SU(3)_2 \to SU(3)_{\text{Color}}$ the scalar becomes an adjoint of the QCD gauge group as described in model A. Because it is charged under $SU(3)_2$ one finds that it's coupling to the axigluon, λ_A of Eq. 2.3, is given by $-g_sG/g$ and thus is automatically enhanced compared to the QCD coupling. In order for the scalar to decay we introduce the dimension 5 operator $\text{tr}\,(\pi G^{\mu\nu}G_{\mu\nu})$ which couples the scalar to two gluons. This operator may be generated by integrating out an additional vector-like pair of fermions charged under $SU(3)_2$ which have

Yukawa coupling to π. These fields could be very heavy so that their only phenomenological consequence is the dimension 5 scalar decay operator.

B Constraints on Axigluons from Dijet Resonance Searches

In this Appendix we consider dijet constraints[1] on axigluon models from UA2 and Tevatron. Since the axigluon can be produced from a $q\overline{q}$ initial state it can also decay into $q\overline{q}$ giving rise to dijet events. Assuming that the axigluon couplings to quarks are flavor-universal ($g_A^q = g_A^t$), the dijet cross section depends on the same parameters m_A, α_A, Γ_A as the $t\bar{t}$ asymmetry and strong constraints can be obtained. In particular, from Table 2.1 and Figure B.1 we see that couplings g_A in the range 0.3 to 0.45 lead to the desired 10% $t\bar{t}$ asymmetry from NP. For such small couplings the axigluon width $\Gamma_A = 5/(24\pi)g_A^2 m_A$ is always negligible (the experimental resolution is on the order of 10%) and narrow resonance searches apply. In Figure B.1 we compare the limits obtained from dijet resonance searches by UA2 [61] and CDF [62] to contours of constant $t\bar{t}$ asymmetry. To obtain these limits we computed the axigluon-mediated dijet cross sections to leading order using MadGraph and compared with the cross section limits quoted by the experiments. We see that over the whole range of masses where searches are available (140-400 GeV) this simplest axigluon explanation of the $t\bar{t}$ asymmetry is inconsistent with dijet constraints. One also sees that the limits are relatively weak for axigluon masses near 280 GeV. Until recently this would have motivated flavor non-universal axigluon models with reduced couplings to first generation quarks and enhanced couplings to top quark to compensate. However such models have been ruled out by LHC searches for pair production of heavy resonances which decay to dijets as discussed in Section 2.3.

[1] For a recent comprehensive review of dijet constraints from hadron colliders see [142].

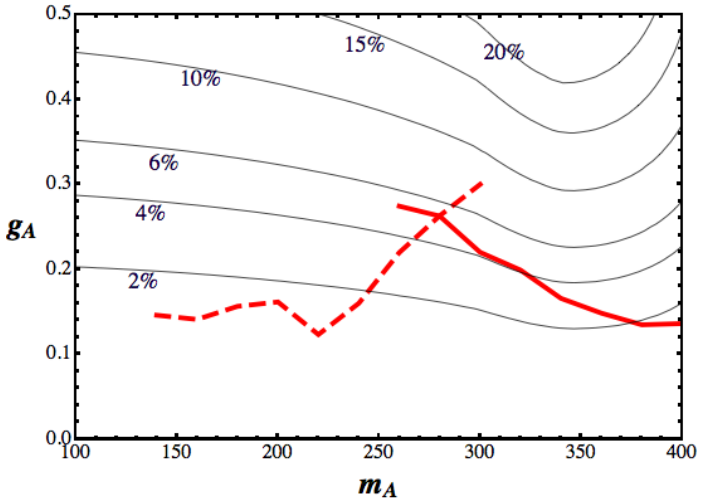

Figure B.1: Contours of constant $t\bar{t}$ asymmetry from axigluon exchange (thin black) versus upper limits on the axigluon coupling g_A from dijet searches at UA2 (dashed red) and CDF (solid red).

C Axigluons and Unitarity

In this Appendix we discuss unitarity constraints on axigluon couplings and demonstrate potential pitfalls with an explicit example (Fig. C.1). Axigluons are massive vector bosons, and in a weakly coupled theory they must arise from a spontaneously broken gauge symmetry. The broken symmetry imposes relations between the coefficients of different terms in the Lagrangian which ensure cancellations between different diagrams when computing scattering amplitudes. These cancellations are required to prevent scattering amplitudes from becoming unphysically large at high energies and spoil unitarity. This is very familiar from the SM where the $e^+e^- \to W^+W^-$ scattering amplitudes from individual diagrams diverge at high energies but are well-behaved once summed together.

In multijet searches unitarity constraints can become especially relevant because many analyses require hard cuts to jet energies in order to suppress QCD backgrounds. These analyses are only sensitive to the high energy tail of axigluon pair production. If one uses an inconsistent model in which unitarity is violated or leaves out some diagrams in the computation of the axigluon signal this tail can be overestimated by orders of magnitude.

At the LHC, to leading order there are two independent axigluon pair production modes. First, axigluons can be produced from a gg initial state as in Fig. 2.5. As discussed in Section III. this cross section is unitary as long as one includes the contribution from the $\mathrm{tr}\,(G^{\mu\nu}[A_\mu, A_\nu])$-term in Eq. 2.2 with $\chi = 1$. This term arises automatically in UV-completions of the theory, e.g. in the models of Appendix A and the two and three site models discussed in [12].

The second axigluon pair production mode at the LHC is from quark-antiquark collisions as in Fig. 2.6. At the 7 or 8 TeV LHC this mode is much smaller than the gg initiated mode except for events with very high invariant mass, when the $q\bar{q}$ parton luminosities become larger than the gg luminosities. Nonetheless the $q\bar{q}$ initial state can be very important because many experimental analyses impose hard cuts suppress QCD background.

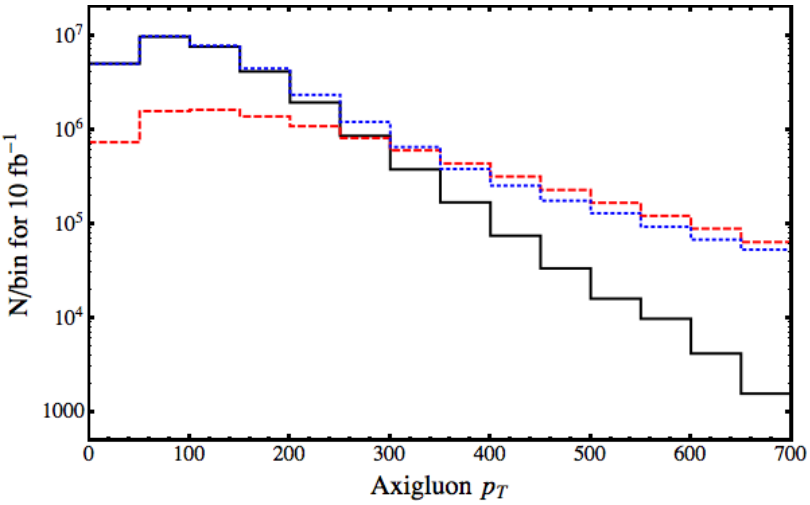

Figure C.1: Leading order differential cross sections for pair production of a 200 GeV axigluon as a function of axigluon p_T at the 7 TeV LHC. The black curve corresponds to a consistent model that includes 150 GeV heavy quarks partners of 1st and 2nd generation quarks and with $\chi = 1$. The red dashed curve corresponds to a model that includes the 150 GeV heavy quarks but with $\chi = 0$. The blue dotted curve corresponds to a model without heavy quarks and with $\chi = 1$. In all 3 models we set $g_A = 0$ and the coupling between a quark and its heavy partner to be equal to g_s.

Phenomenological studies for such analyses must employ simulations with both gg and $q\bar{q}$ initial states, and one must be careful to use a model with consistent quark couplings to axigluons. As we explain in the following paragraphs this requires the existence of new heavy fermions, and their contributions to axigluon pair production at high energies cannot be ignored.

We showed in section III that the coupling of axigluons to SM quarks must be less than the QCD gauge coupling g_s in order to explain the $t\bar{t}$ asymmetry. Small axial couplings of axigluons to quarks can be obtained through fermion mixing thus requiring heavy fermion partners (to mix with). These heavy fermions contribute to axigluon pair production through t-channel exchange as shown in Fig. 2.6 (c). Neglecting these contributions produces unphysical cross-sections which violate unitarity. Moreover, in the absence of a parity symmetry there is also a contribution from a vertex with 3 axigluons as shown in

Fig. 2.6 (d).

In Fig. C.1 we show the cross sections for axigluon pair production at the LHC for the parity symmetric model of Appendix A (black curve) and for two inconsistent models (blue and red curves). The plot illustrates the unphysical growth of amplitudes in inconsistent models. The blue curve corresponds to a model with $\chi = 1$ but without heavy partners for the light quarks. Hence the contribution from the diagram in Fig. 2.6 (c) is missing, and there is a large enhancement of the partonic cross section $q\bar{q} \to AA$ at high energies (the cross section falls after convolution with the parton distribution functions but the amplitude actually grows in this model). In Fig. C.1 this results in an increase by more than a order of magnitude of the axigluon pair production cross section at high p_T. The red curve corresponds to a model that includes heavy quark partners consistently but which has $\chi = 0$. In this model both the $gg \to AA$ and $q\bar{q} \to AA$ amplitudes violate unitarity at high energies. In addition, the coupling proportional to χ also has an important effect on the $gg \to AA$ amplitude at low energies so that setting $\chi = 0$ results in a significant *underestimate* of the cross section near threshold.

Bibliography

[1] **CMS** Collaboration, C. Collaboration, *Differential measurements of the charge asymmetry in top quark pair production*, .

[2] **ATLAS** Collaboration, G. Aad et al., *Search for Massive Colored Scalars in Four-Jet Final States in $\sqrt{s} = 7$ TeV proton-proton collisions with the ATLAS Detector*, *The European Physical Journal* **C71** (2011) 1828, [arXiv:1110.2693].

[3] **ATLAS** Collaboration, *Search for Massive Coloured Scalars with the ATLAS Detector in Four-Jet Final States using 4.6 fb^{-1} of $\sqrt{s} = 7$ TeV proton-proton collision data*, .

[4] **CMS** Collaboration, S. Chatrchyan et al., *Search for pair-produced dijet resonances in four-jet final states in pp collisions at $\sqrt{s} = 7$??TeV*, *Physical Review Letters* **110** (2013), no. 14 141802, [arXiv:1302.0531].

[5] **CMS** Collaboration, S. Chatrchyan et al., *Observation of a new boson at a mass of 125 GeV with the CMS experiment at the LHC*, *Physics Letters* **B716** (2012) 30–61, [arXiv:1207.7235].

[6] **ATLAS** Collaboration, G. Aad et al., *Observation of a new particle in the search for the Standard Model Higgs boson with the ATLAS detector at the LHC*, *Physics Letters* **B716** (2012) 1–29, [arXiv:1207.7214].

[7] S. Glashow, *Partial Symmetries of Weak Interactions*, *Nuclear Physics* **22** (1961) 579–588.

[8] S. Weinberg, *A Model of Leptons*, *Physical Review Letters* **19** (1967) 1264–1266.

[9] A. Salam, *Weak and Electromagnetic Interactions*, *Svartholm: Elementary Particle Theory, Proceedings Of The Nobel Symposium Held 1968 At Lerum, Sweden* (1968).

[10] **D0** Collaboration, V. M. Abazov et al., *Forward-backward asymmetry in top quark-antiquark production*, *Physical Review* **D84** (2011) 112005, [arXiv:1107.4995].

[11] **CDF** Collaboration, T. Aaltonen et al., *Measurement of the top quark forward-backward production asymmetry and its dependence on event kinematic properties*, *Physical Review* **D87** (2013), no. 9 092002, [arXiv:1211.1003].

[12] G. Marques Tavares and M. Schmaltz, *Explaining the t-tbar asymmetry with a light axigluon*, *Physical Review* **D84** (2011) 054008, [arXiv:1107.0978].

[13] C. Gross, G. Marques Tavares, M. Schmaltz, and C. Spethmann, *Light axigluon explanation of the Tevatron $t\bar{t}$ asymmetry and multijet signals at the LHC*, *Physical Review* **D87** (2013), no. 1 014004, [arXiv:1209.6375].

[14] S. P. Martin, *A Supersymmetry primer*, *Advanced Series on Directions in High Energy Physics* **21** (2010) 1–153, [hep-ph/9709356].

[15] R. Contino, *The Higgs as a Composite Nambu-Goldstone Boson*, arXiv:1005.4269.

[16] W. A. Bardeen, *On naturalness in the standard model*, .

[17] G. Marques Tavares, M. Schmaltz, and W. Skiba, *Higgs mass naturalness and scale invariance in the UV*, *Physical Review* **D89** (2014), no. 1 015009, [arXiv:1308.0025].

[18] E. W. Kolb and M. S. Turner, *The Early Universe*, vol. 69. Frontiers in Physics, 1990.

[19] J. H. Kuhn and G. Rodrigo, *Charge asymmetry in hadroproduction of heavy quarks*, *Physical Review Letters* **81** (1998) 49–52, [hep-ph/9802268].

[20] J. H. Kuhn and G. Rodrigo, *Charge asymmetry of heavy quarks at hadron colliders*, *Physical Review* **D59** (1999) 054017, [hep-ph/9807420].

[21] M. Bowen, S. Ellis, and D. Rainwater, *Standard model top quark asymmetry at the Fermilab Tevatron*, *Physical Review* **D73** (2006) 014008, [hep-ph/0509267].

[22] L. G. Almeida, G. F. Sterman, and W. Vogelsang, *Threshold Resummation for the Top Quark Charge Asymmetry*, *Physical Review* **D78** (2008) 014008, [arXiv:0805.1885].

[23] **CDF** Collaboration, *Measurement of the Forward Backward Asymmetry in Top Pair Production in the Dilepton Decay Channel using 5.1 $fb^{?1}$*, .

[24] **CDF** Collaboration, *Combined result of the Forward Backward Asymmetry in Top Pair Production from Lepton Plus Jet and Di-lepton Channels Using Data up to 5.3 fb^{-1}*, .

[25] **CDF** Collaboration, T. Aaltonen et al., *Evidence for a Mass Dependent Forward-Backward Asymmetry in Top Quark Pair Production*, *Physical Review* **D83** (2011) 112003, [arXiv:1101.0034].

[26] **D0** Collaboration, V. M. Abazov et al., *Measurement of Leptonic Asymmetries and Top Quark Polarization in $t\bar{t}$ Production*, *Physical Review* **D87** (2013), no. 1 011103, [arXiv:1207.0364].

[27] P. H. Frampton and S. L. Glashow, *Chiral Color: An Alternative to the Standard Model*, *Physics Letters* **B190** (1987) 157.

[28] P. H. Frampton, J. Shu, and K. Wang, *Axigluon as Possible Explanation for p anti-p $---->$ t anti-t Forward-Backward Asymmetry*, *Physics Letters* **B683** (2010) 294–297, [arXiv:0911.2955].

[29] B. Xiao, Y.-k. Wang, and S.-h. Zhu, *New Color-Octet Vector Boson?*, arXiv:1011.0152.

[30] R. Barcelo, A. Carmona, M. Masip, and J. Santiago, *Stealth gluons at hadron colliders*, *Physics Letters* **B707** (2012) 88–91, [arXiv:1106.4054].

[31] J. Aguilar-Saavedra and M. Perez-Victoria, *Shaping the top asymmetry*, *Physics Letters* **B705** (2011) 228–234, [arXiv:1107.2120].

[32] G. Z. Krnjaic, *Very Light Axigluons and the Top Asymmetry*, *Physical Review* **D85** (2012) 014030, [arXiv:1109.0648].

[33] J. Drobnak, J. F. Kamenik, and J. Zupan, *Flipping t tbar Asymmetries at the Tevatron and the LHC*, *Physical Review* **D86** (2012) 054022, [arXiv:1205.4721].

[34] S. Dutta, A. Goyal, and M. Kumar, *Top quark physics in the vector color-octet model*, *Physical Review* **D87** (2013), no. 9 094016, [arXiv:1209.3636].

[35] E. Alvarez and E. C. Leskow, *A charged Z' to conciliate the apparent disagreement between top-antitop Tevatron forward-backward asymmetry and LHC charge asymmetry*, *Physical Review* **D86** (2012) 114034, [arXiv:1209.4354].

[36] J. Drobnak, A. L. Kagan, J. F. Kamenik, G. Perez, and J. Zupan, *Forward Tevatron Tops and Backward LHC Tops with Associates*, *Physical Review* **D86** (2012) 094040, [arXiv:1209.4872].

[37] S. Jung, A. Pierce, and J. D. Wells, *Top quark asymmetry from a non-Abelian horizontal symmetry*, *Physical Review* **D83** (2011) 114039, [arXiv:1103.4835].

[38] **ATLAS** Collaboration, G. Aad et al., *Measurements of top quark pair relative differential cross-sections with ATLAS in pp collisions at* $\sqrt{s} = 7$ *TeV*, *The European Physical Journal* **C73** (2013), no. 1 2261, [arXiv:1207.5644].

[39] M. I. Gresham, I.-W. Kim, and K. M. Zurek, *On Models of New Physics for the Tevatron Top* A_{FB}, *Physical Review* **D83** (2011) 114027, [arXiv:1103.3501].

[40] J. Aguilar-Saavedra and M. Perez-Victoria, *Simple models for the top asymmetry: Constraints and predictions*, *Journal of High Energy Physics* **1109** (2011) 097, [arXiv:1107.0841].

[41] M. I. Gresham, I.-W. Kim, and K. M. Zurek, *Tevatron Top A_{FB} Versus LHC Top Physics*, *Physical Review* **D85** (2012) 014022, [arXiv:1107.4364].

[42] M. I. Gresham, I.-W. Kim, S. Tulin, and K. M. Zurek, *Confronting Top AFB with Parity Violation Constraints*, *Physical Review* **D86** (2012) 034029, [arXiv:1203.1320].

[43] **CMS** Collaboration, S. Chatrchyan et al., *Search for new physics in events with same-sign dileptons and b-tagged jets in pp collisions at $\sqrt{s} = 7$ TeV*, *Journal of High Energy Physics* **1208** (2012) 110, [arXiv:1205.3933].

[44] J. Aguilar-Saavedra and J. Santiago, *Four tops and the $t\bar{t}$ forward-backward asymmetry*, *Physical Review* **D85** (2012) 034021, [arXiv:1112.3778].

[45] G. M. Tavares, "Madgraph Axigluon Models." http://physics.bu.edu/~gusmt/axigluon, 2012.

[46] J. Alwall, M. Herquet, F. Maltoni, O. Mattelaer, and T. Stelzer, *MadGraph 5 : Going Beyond*, *Journal of High Energy Physics* **1106** (2011) 128, [arXiv:1106.0522].

[47] N. D. Christensen and C. Duhr, *FeynRules - Feynman rules made easy*, *Computer Physics Communications* **180** (2009) 1614–1641, [arXiv:0806.4194].

[48] U. Haisch and S. Westhoff, *Massive Color-Octet Bosons: Bounds on Effects in Top-Quark Pair Production*, *Journal of High Energy Physics* **1108** (2011) 088, [arXiv:1106.0529].

[49] **ATLAS** Collaboration, *Measurement of the charge asymmetry in dileptonic decay of top quark pairs in pp collisions at s = 7 TeV using the ATLAS detector*, .

[50] **CDF** Collaboration, *'Combination of CDF top quark pair production cross section measurements with up to 4.6 fb - 1,*, .

[51] **D0** Collaboration, V. M. Abazov et al., *Measurement of the top quark pair production cross section in the lepton+jets channel in proton-antiproton collisions at $\sqrt{s}$=1.96 TeV*, *Physical Review* **D84** (2011) 012008, [arXiv:1101.0124].

[52] **CMS** Collaboration, S. Chatrchyan et al., *Measurement of the $t\bar{t}$ production cross section in the dilepton channel in pp collisions at $\sqrt{s} = 7$ TeV*, *Journal of High Energy Physics* **1211** (2012) 067, [arXiv:1208.2671].

[53] **ATLAS** Collaboration, *Measurement of the top quark pair production cross-section with ATLAS in pp collisions at $\sqrt{s} = 7$ TeV in the single-lepton channel using semileptonic b decays*, .

[54] Y. Bai and Z. Han, *Improving the Top Quark Forward-Backward Asymmetry Measurement at the LHC*, *Journal of High Energy Physics* **1202** (2012) 135, [arXiv:1106.5071].

[55] J.-F. Arguin, M. Freytsis, and Z. Ligeti, *Comment on measuring the t-tbar forward-backward asymmetry at ATLAS and CMS*, *Physical Review* **D84** (2011) 071504, [arXiv:1107.4090].

[56] J. Aguilar-Saavedra, A. Juste, and F. Rubbo, *Boosting the t tbar charge asymmetry*, *Physics Letters* **B707** (2012) 92–98, [arXiv:1109.3710].

[57] E. L. Berger, Q.-H. Cao, C.-R. Chen, and H. Zhang, *Interpretations and implications of the top quark rapidity asymmetries A^t_{FB} and A^l_{FB}*, *Physical Review* **D88** (2013), no. 1 014033, [arXiv:1209.4899].

[58] A. Falkowski, G. Perez, and M. Schmaltz, *Spinning the top quark*, *Physical Review* **D87** (2013), no. 3 034041, [arXiv:1110.3796].

[59] C. Kilic, S. Schumann, and M. Son, *Searching for Multijet Resonances at the LHC*, *Journal of High Energy Physics* **0904** (2009) 128, [arXiv:0810.5542].

[60] R. Essig, *Physics beyond the standard model: Supersymmetry, dark matter, and LHC phenomenology*, .

[61] **UA2 Collaboration** Collaboration, J. Alitti et al., *A Search for new intermediate vector mesons and excited quarks decaying to two jets at the CERN $\bar{p}p$ collider*, *Nuclear Physics* **B400** (1993) 3–24.

[62] **CDF** Collaboration, T. Aaltonen et al., *Search for new particles decaying into dijets in proton-antiproton collisions at s**(1/2) = 1.96-TeV*, *Physical Review* **D79** (2009) 112002, [arXiv:0812.4036].

[63] **CDF** Collaboration, T. Aaltonen et al., *Search for Higgs Bosons Produced in Association with b-quarks*, *Physical Review* **D85** (2012) 032005, [arXiv:1106.4782].

[64] Z. Hubacek, *Measurement of the Three-jet Mass Cross Section in $p\bar{p}$ Collisions at $\sqrt{s} = 1.96$ TeV*, .

[65] **CMS** Collaboration, *Search for Black Holes in pp Collisions at sqrt(s) = 7 TeV*, .

[66] **CMS** Collaboration, C. Collaboration, *Search for Multijet Resonances in the 8-jet Final State*, .

[67] J. Butterworth, B. Cox, and J. R. Forshaw, *WW scattering at the CERN LHC*, *Physical Review* **D65** (2002) 096014, [hep-ph/0201098].

[68] J. M. Butterworth, A. R. Davison, M. Rubin, and G. P. Salam, *Jet substructure as a new Higgs search channel at the LHC*, *Physical Review Letters* **100** (2008) 242001, [arXiv:0802.2470].

[69] L. G. Almeida, S. J. Lee, G. Perez, G. F. Sterman, I. Sung, et al., *Substructure of high-p_T Jets at the LHC*, *Physical Review* **D79** (2009) 074017, [arXiv:0807.0234].

[70] D. Krohn, J. Thaler, and L.-T. Wang, *Jet Trimming*, *Journal of High Energy Physics* **1002** (2010) 084, [arXiv:0912.1342].

[71] S. D. Ellis, C. K. Vermilion, and J. R. Walsh, *Techniques for improved heavy particle searches with jet substructure*, *Physical Review* **D80** (2009) 051501, [arXiv:0903.5081].

[72] D. E. Kaplan, K. Rehermann, M. D. Schwartz, and B. Tweedie, *Top Tagging: A Method for Identifying Boosted Hadronically Decaying Top Quarks*, *Physical Review Letters* **101** (2008) 142001, [arXiv:0806.0848].

[73] J. Thaler and K. Van Tilburg, *Identifying Boosted Objects with N-subjettiness*, *Journal of High Energy Physics* **1103** (2011) 015, [arXiv:1011.2268].

[74] J. Thaler and K. Van Tilburg, *Maximizing Boosted Top Identification by Minimizing N-subjettiness*, *Journal of High Energy Physics* **1202** (2012) 093, [arXiv:1108.2701].

[75] Y. Bai and J. Shelton, *Composite Octet Searches with Jet Substructure*, *Journal of High Energy Physics* **1207** (2012) 067, [arXiv:1107.3563].

[76] M. Son, C. Spethmann, and B. Tweedie, *Diboson-Jets and the Search for Resonant Zh Production*, *Journal of High Energy Physics* **1208** (2012) 160, [arXiv:1204.0525].

[77] J. Sayre, D. A. Dicus, C. Kao, and S. Nandi, *Searching for Colorons at the Large Hadron Collider*, *Physical Review* **D84** (2011) 015011, [arXiv:1105.3219].

[78] **CDF** Collaboration, T. Aaltonen et al., *First Search for Multijet Resonances in* $\sqrt{s} = 1.96$ *TeV* $p\bar{p}$ *Collisions*, *Physical Review Letters* **107** (2011) 042001, [arXiv:1105.2815].

[79] **CMS** Collaboration, S. Chatrchyan et al., *Search for Three-Jet Resonances in pp Collisions at* $\sqrt{s} = 7$ *TeV*, *Physical Review Letters* **107** (2011) 101801, [arXiv:1107.3084].

[80] P. A. Dirac, *The Cosmological constants*, *Nature* **139** (1937) 323.

[81] P. A. Dirac, *New basis for cosmology*, *Proceedings of the Royal Society* **A165** (1938) 199–208.

[82] G. 't Hooft, *Naturalness, chiral symmetry, and spontaneous chiral symmetry breaking*, *Nato Science Series B* **59** (1980) 135.

[83] M. A. Luty, J. Polchinski, and R. Rattazzi, *The a-theorem and the Asymptotics of 4D Quantum Field Theory*, *Journal of High Energy Physics* **1301** (2013) 152, [arXiv:1204.5221].

[84] J.-F. Fortin, B. Grinstein, and A. Stergiou, *Limit Cycles and Conformal Invariance*, *Journal of High Energy Physics* **1301** (2013) 184, [arXiv:1208.3674].

[85] K. A. Meissner and H. Nicolai, *Conformal Symmetry and the Standard Model*, *Physics Letters* **B648** (2007) 312–317, [hep-th/0612165].

[86] W.-F. Chang, J. N. Ng, and J. M. Wu, *Shadow Higgs from a scale-invariant hidden U(1)(s) model*, *Physical Review* **D75** (2007) 115016, [hep-ph/0701254].

[87] R. Foot, A. Kobakhidze, K. McDonald, and R. Volkas, *Neutrino mass in radiatively-broken scale-invariant models*, *Physical Review* **D76** (2007) 075014, [arXiv:0706.1829].

[88] T. Hambye and M. H. Tytgat, *Electroweak symmetry breaking induced by dark matter*, *Physics Letters* **B659** (2008) 651–655, [arXiv:0707.0633].

[89] R. Foot, A. Kobakhidze, K. L. McDonald, and R. R. Volkas, *A Solution to the hierarchy problem from an almost decoupled hidden sector within a classically scale invariant theory*, *Physical Review* **D77** (2008) 035006, [arXiv:0709.2750].

[90] M. Shaposhnikov and D. Zenhausern, *Quantum scale invariance, cosmological constant and hierarchy problem*, *Physics Letters* **B671** (2009) 162–166, [arXiv:0809.3406].

[91] S. Iso, N. Okada, and Y. Orikasa, *Classically conformal B^- L extended Standard Model*, *Physics Letters* **B676** (2009) 81–87, [arXiv:0902.4050].

[92] K. A. Meissner and H. Nicolai, *Conformal invariance from non-conformal gravity*, *Physical Review* **D80** (2009) 086005, [arXiv:0907.3298].

[93] M. Holthausen, M. Lindner, and M. A. Schmidt, *Radiative Symmetry Breaking of the Minimal Left-Right Symmetric Model*, *Physical Review* **D82** (2010) 055002, [arXiv:0911.0710].

[94] R. Foot, A. Kobakhidze, and R. R. Volkas, *Stable mass hierarchies and dark matter from hidden sectors in the scale-invariant standard model*, *Physical Review* **D82** (2010) 035005, [arXiv:1006.0131].

[95] L. Alexander-Nunneley and A. Pilaftsis, *The Minimal Scale Invariant Extension of the Standard Model*, *Journal of High Energy Physics* **1009** (2010) 021, [arXiv:1006.5916].

[96] T. Hur and P. Ko, *Scale invariant extension of the standard model with strongly interacting hidden sector*, *Physical Review Letters* **106** (2011) 141802, [arXiv:1103.2571].

[97] A. R. Vieira, B. Hiller, M. D. Sampaio, and M. Nemes, *Naturalness and Theoretical Constraints on the Higgs Boson Mass*, *International Journal of Theoretical Physics* **52** (2013) 3494–3503, [arXiv:1207.4088].

[98] S. Iso and Y. Orikasa, *TeV Scale B-L model with a flat Higgs potential at the Planck scale - in view of the hierarchy problem -*, *Progress of Theoretical and Experimental Physics* **2013** (2013) 023B08, [arXiv:1210.2848].

[99] C. Englert, J. Jaeckel, V. Khoze, and M. Spannowsky, *Emergence of the Electroweak Scale through the Higgs Portal*, *Journal of High Energy Physics* **1304** (2013) 060, [arXiv:1301.4224].

[100] M. Fabbrichesi and S. Petcov, *Low-scale neutrino seesaw mechanism and scalar dark matter*, *The European Physical Journal* **C74** (2014) 2774, [arXiv:1304.4001].

[101] Y. Orikasa, *Classically conformal B-L extended Standard Model and phenomenology*, arXiv:1304.4700.

[102] M. Heikinheimo, A. Racioppi, M. Raidal, C. Spethmann, and K. Tuominen, *Physical Naturalness and Dynamical Breaking of Classical Scale Invariance*, *Modern Physics Letters* **A29** (2014) 1450077, [arXiv:1304.7006].

[103] I. Oda, *Classically Scale-invariant B-L Model and Conformal Gravity*, *Physics Letters* **B724** (2013) 160–164, [arXiv:1305.0884].

[104] S. Dubovsky, V. Gorbenko, and M. Mirbabayi, *Natural Tuning: Towards A Proof of Concept*, *Journal of High Energy Physics* **1309** (2013) 045, [arXiv:1305.6939].

[105] V. V. Khoze and G. Ro, *Leptogenesis and Neutrino Oscillations in the Classically Conformal Standard Model with the Higgs Portal*, *Journal of High Energy Physics* **1310** (2013) 075, [arXiv:1307.3764].

[106] D. Gorbunov and A. Tokareva, *Scale-invariance as the origin of dark radiation?*, *Physics Letters* **B739** (2014) 50–55, [arXiv:1307.5298].

[107] C. D. Carone and R. Ramos, *Classical scale-invariance, the electroweak scale and vector dark matter*, *Physical Review* **D88** (2013) 055020, [arXiv:1307.8428].

[108] A. Farzinnia, H.-J. He, and J. Ren, *Natural Electroweak Symmetry Breaking from Scale Invariant Higgs Mechanism*, *Physics Letters* **B727** (2013) 141–150, [arXiv:1308.0295].

[109] P. H. Frampton and C. Vafa, *Conformal approach to particle phenomenology*, hep-th/9903226.

[110] C. Csaki, W. Skiba, and J. Terning, *Beta functions of orbifold theories and the hierarchy problem*, *Physical Review* **D61** (2000) 025019, [hep-th/9906057].

[111] T. Banks and A. Zaks, *On the Phase Structure of Vector-Like Gauge Theories with Massless Fermions*, *Nuclear Physics* **B196** (1982) 189.

[112] G. Leibbrandt, *Introduction to the Technique of Dimensional Regularization*, *Review of Modern Physics* **47** (1975) 849.

[113] M. E. Peskin and D. V. Schroeder, *An Introduction to quantum field theory*. Addison-Wesley, 1993.

[114] **Planck** Collaboration, P. Ade et al., *Planck 2015 results. XIII. Cosmological parameters*, arXiv:1502.01589.

[115] J. L. Feng, H. Tu, and H.-B. Yu, *Thermal Relics in Hidden Sectors*, *Journal of Cosmology and Astroparticle Physics* **0810** (2008) 043, [arXiv:0808.2318].

[116] J. L. Feng, M. Kaplinghat, H. Tu, and H.-B. Yu, *Hidden Charged Dark Matter*, *Journal of Cosmology and Astroparticle Physics* **0907** (2009) 004, [arXiv:0905.3039].

[117] R. Diamanti, E. Giusarma, O. Mena, M. Archidiacono, and A. Melchiorri, *Dark Radiation and interacting scenarios*, *Physical Review* **D87** (2013), no. 6 063509, [arXiv:1212.6007].

[118] S. Hofmann, D. J. Schwarz, and H. Stoecker, *Damping scales of neutralino cold dark matter*, *Physical Review* **D64** (2001) 083507, [astro-ph/0104173].

[119] **BOSS Collaboration** Collaboration, F. Beutler et al., *The clustering of galaxies in the SDSS-III Baryon Oscillation Spectroscopic Survey: Signs of neutrino mass in current cosmological datasets*, *Monthly Notices of the Royal Astronomical Society* **444** (2014) 3501, [arXiv:1403.4599].

[120] R. A. Battye, T. Charnock, and A. Moss, *Tension between the power spectrum of density perturbations measured on large and small scales*, arXiv:1409.2769.

[121] M. Ibe, S. Matsumoto, and R. Sato, *Mass Splitting between Charged and Neutral Winos at Two-Loop Level*, *Physics Letters* **B721** (2013) 252–260, [arXiv:1212.5989].

[122] M. Cirelli, N. Fornengo, and A. Strumia, *Minimal dark matter*, *Nuclear Physics* **B753** (2006) 178–194, [hep-ph/0512090].

[123] M. Cirelli, A. Strumia, and M. Tamburini, *Cosmology and Astrophysics of Minimal Dark Matter*, *Nuclear Physics* **B787** (2007) 152–175, [arXiv:0706.4071].

[124] R. J. Hill and M. P. Solon, *WIMP-nucleon scattering with heavy WIMP effective theory*, *Physical Review Letters* **112** (2014) 211602, [arXiv:1309.4092].

[125] P. Cushman, C. Galbiati, D. McKinsey, H. Robertson, T. Tait, et al., *Working Group Report: WIMP Dark Matter Direct Detection*, arXiv:1310.8327.

[126] M. Low and L.-T. Wang, *Neutralino dark matter at 14 TeV and 100 TeV*, *Journal of High Energy Physics* **1408** (2014) 161, [arXiv:1404.0682].

[127] M. Cirelli, F. Sala, and M. Taoso, *Wino-like Minimal Dark Matter and future colliders*, *Journal of High Energy Physics* **1410** (2014) 033, [arXiv:1407.7058].

[128] D. S. M. Alves, J. Galloway, J. T. Ruderman, and J. R. Walsh, *Running Electroweak Couplings as a Probe of New Physics*, *Journal of High Energy Physics* **1502** (2015) 007, [arXiv:1410.6810].

[129] T. Cohen, M. Lisanti, A. Pierce, and T. R. Slatyer, *Wino Dark Matter Under Siege*, *Journal of Cosmology and Astroparticle Physics* **1310** (2013) 061, [arXiv:1307.4082].

[130] J. Fan and M. Reece, *In Wino Veritas? Indirect Searches Shed Light on Neutralino Dark Matter*, *Journal of High Energy Physics* **1310** (2013) 124, [arXiv:1307.4400].

[131] G. Ovanesyan, T. R. Slatyer, and I. W. Stewart, *Heavy Dark Matter Annihilation from Effective Field Theory*, arXiv:1409.8294.

[132] M. Baumgart, I. Z. Rothstein, and V. Vaidya, *Constraints on Galactic Wino Densities from Gamma Ray Lines*, arXiv:1412.8698.

[133] S. Funk, *Indirect Detection of Dark Matter with gamma rays*, arXiv:1310.2695.

[134] W. Hu, D. J. Eisenstein, M. Tegmark, and M. J. White, *Observationally determining the properties of dark matter*, *Physical Review* **D59** (1999) 023512, [astro-ph/9806362].

[135] R. Bowen, S. H. Hansen, A. Melchiorri, J. Silk, and R. Trotta, *The Impact of an extra background of relativistic particles on the cosmological parameters derived from microwave background anisotropies*, *Monthly Notices of the Royal Astronomical Society* **334** (2002) 760, [astro-ph/0110636].

[136] S. Bashinsky and U. Seljak, *Neutrino perturbations in CMB anisotropy and matter clustering*, *Physical Review* **D69** (2004) 083002, [astro-ph/0310198].

[137] A. Friedland, K. M. Zurek, and S. Bashinsky, *Constraining Models of Neutrino Mass and Neutrino Interactions with the Planck Satellite*, arXiv:0704.3271.

[138] R. J. Wilkinson, C. Boehm, and J. Lesgourgues, *Constraining Dark Matter-Neutrino Interactions using the CMB and Large-Scale Structure*, *Journal of Cosmology and Astroparticle Physics* **1405** (2014) 011, [arXiv:1401.7597].

[139] S. D. McDermott, H.-B. Yu, and K. M. Zurek, *Turning off the Lights: How Dark is Dark Matter?*, *Physical Review* **D83** (2011) 063509, [arXiv:1011.2907].

[140] C.-P. Ma and E. Bertschinger, *Cosmological perturbation theory in the synchronous and conformal Newtonian gauges*, *Astrophysical Journal* **455** (1995) 7–25, [astro-ph/9506072].

[141] C. Dvorkin, K. Blum, and M. Kamionkowski, *Constraining Dark Matter-Baryon Scattering with Linear Cosmology*, *Physical Review* **D89** (2014), no. 2 023519, [arXiv:1311.2937].

[142] R. M. Harris and K. Kousouris, *Searches for Dijet Resonances at Hadron Colliders*, *International Journal of Modern Physics* **A26** (2011) 5005–5055, [arXiv:1110.5302].

Curriculum Vitae

Gustavo Marques Tavares

Personal Data

Name: Gustavo Marques Tavares
Date of birth: 1985, April 30
Citizenship: Brazilian
Professional Address: Physics Department, Boston University,
590 Commonwealth Ave,
Boston, MA 02215
E-mail: gusmt@bu.edu

Education

Boston University, Boston, Massachusetts, USA
Ph.D. in Physics *Expected: May 2015*

Universidade Estadual de Campinas, Campinas, Sao Paulo, Brazil
M.Sc. in Physics *April 2010*

Universidade Estadual de Campinas, Campinas, Sao Paulo, Brazil
B.Sc. in Physics *January 2008*

Fellowships and Awards

- DOE Graduate Fellowship in High Energy Theory, 2012.
- LHC Theory Initiative Graduate Fellowship, 2012.
- The Gertrude and Maurice Goldhaber Award in Physics, Boston University, 2011.
- CAPES/FIPSE Fellowship for exchange program with Caltech, 2006.

Publications

- E. Katz, G. Marques Tavares, and Y. Xu, "A solution of 2D QCD at Finite N using a conformal basis," `arXiv:1405.6727 [hep-th]`
- A. Cohen, G. Marques Tavares, and Y. Xu, "Seeking Lorentz Violation from the Higgs," `arXiv:1404.3185 [hep-ph]`
- E. Katz, G. Marques Tavares, and Y. Xu, "Solving 2D QCD with an adjoint fermion analytically," *JHEP* **1405** (2014) 143, `arXiv:1308.4980 [hep-th]`
- G. Marques Tavares, M. Schmaltz, and W. Skiba, "Higgs mass naturalness and scale invariance in the UV," *Phys.Rev.* **D89** (2014) 015009, `arXiv:1308.0025 [hep-ph]`

- C. Gross, G. Marques Tavares, M. Schmaltz, and C. Spethmann, "Light axigluon explanation of the Tevatron ttbar asymmetry and multijet signals at the LHC," *Phys.Rev.* **D87** (2013) 014004, `arXiv:1209.6375 [hep-ph]`
- G. Marques Tavares and M. Schmaltz, "Explaining the t-tbar asymmetry with a light axigluon," *Phys.Rev.* **D84** (2011) 054008, `arXiv:1107.0978 [hep-ph]`
- Z. Ligeti, G. Marques Tavares, and M. Schmaltz, "Explaining the t tbar forward-backward asymmetry without dijet or flavor anomalies," *JHEP* **1106** (2011) 109, `arXiv:1103.2757 [hep-ph]`
- R. A. Mosna and G. Marques Tavares, "New self-dual solutions of SU(2) Yang-Mills theory in Euclidean Schwarzschild space," *Phys.Rev.* **D80** (2009) 105006, `arXiv:0909.5145 [math-ph]`

Conferences and Workshops

- *Phenomenology Symposium*, 2014;
  University of Pittsburgh, Pittsburgh, PA.
- *Beyond the Standard Model after the first run of the LHC*, 2013;
  The Galileo Galilei Institute for Theoretical Physics, Florence, Italy.
- *LHC Theory Initiative Meeting*, 2013;
  Stony Brook University, Stony Brook, NY.
- *The first year of the LHC*, 2011 - Affiliate member;
  The Kavli Institute for Theoretical Physics, Santa Barbara, CA.

Seminars and Presentations

- *Non-Abelian Dark Matter and Dark Radiation*, MIT, February 2015.
- *Non-Abelian Dark Matter*, UC Davis, November 2014.
- *Non-Abelian Dark Matter*, LBNL, November 2014.
- *Seeking Lorentz violations from the Higgs*, Johns Hopkins University, September 2014.
- *Seeking Lorentz violations from the Higgs*, University of Maryland, September 2014.
- *Seeking Lorentz violations from the Higgs*, Phenomenology Symposium, May 2014.
- *Higgs mass naturalness and scale invariance in the UV*, MIT, February 2014.
- $t\bar{t}$ *asymmetry, axigluons and multijets at the LHC*, LHC Theory Initiative Meeting, February 2013.